

The diagram illustrates a digital magnetic recording system. The input signal I_n is processed by an Encoder (Rate 9/8), a Serializer, and a Precoder. The output of the Precoder is sent to the Write/Read Head, which is connected to a Disk. The output from the Disk is received by Arm Electronics, then passes through a VGA, an Analog LPF, and an A/D converter. The A/D output x_n is processed by a Digital Equalizer and a Timing Recovery & Gain Control block. The Timing Recovery & Gain Control block also receives feedback from the output of the Decoder (Rate 9/8) and provides control signals to the A/D converter and the Digital Equalizer. The output of the Digital Equalizer is y_n , which is fed into an NPML Detector, an Inverse Precoder, a De-serializer, and finally a Decoder (Rate 9/8) to produce the final output $n-d$. The diagram is labeled with various components and signals, including I_n , x_n , y_n , $n-d$, and control signals A, B, and C.

FOR THE PURPOSES OF INFORMATION ONLY

Codes used to identify States party to the PCT on the front pages of pamphlets publishing international applications under the PCT.

AM	Armenia	GB	United Kingdom	MW	Malawi
AT	Austria	GE	Georgia	MX	Mexico
AU	Australia	GN	Guinea	NE	Niger
BB	Barbados	GR	Greece	NL	Netherlands
BE	Belgium	HU	Hungary	NO	Norway
BF	Burkina Faso	IE	Ireland	NZ	New Zealand
BG	Bulgaria	IT	Italy	PL	Poland
BJ	Benin	JP	Japan	PT	Portugal
BR	Brazil	KE	Kenya	RO	Romania
BY	Belarus	KG	Kyrgyzstan	RU	Russian Federation
CA	Canada	KP	Democratic People's Republic of Korea	SD	Sudan
CF	Central African Republic			SE	Sweden
CG	Congo	KR	Republic of Korea	SG	Singapore
CH	Switzerland	KZ	Kazakhstan	SI	Slovenia
CI	Côte d'Ivoire	LI	Liechtenstein	SK	Slovakia
CM	Cameroon	LK	Sri Lanka	SN	Senegal
CN	China	LR	Liberia	SZ	Swaziland
CS	Czechoslovakia	LT	Lithuania	TD	Chad
CZ	Czech Republic	LU	Luxembourg	TG	Togo
DE	Germany	LV	Latvia	TJ	Tajikistan
DK	Denmark	MC	Monaco	TT	Trinidad and Tobago
EE	Estonia	MD	Republic of Moldova	UA	Ukraine
ES	Spain	MG	Madagascar	UG	Uganda
FI	Finland	ML	Mali	US	United States of America
FR	France	MN	Mongolia	UZ	Uzbekistan
GA	Gabon	MR	Mauritania	VN	Viet Nam

DESCRIPTION

APPARATUS AND METHOD FOR NOISE-PREDICTIVE MAXIMUM-LIKELIHOOD (NPML) DETECTION

TECHNICAL FIELD

10 The invention relates to data detection methods and apparatus, particularly methods and apparatus for partial-response signaling and maximum-likelihood sequence detection. It further relates to direct access storage devices (DASDs) based on these methods.

15 BACKGROUND OF THE INVENTION

Application of partial-response (PR) class-IV (PR4) equalization and maximum likelihood sequence detection (MLSD) has been shown in theory and practice to achieve near optimal performance at recording densities of
20 $0.8 \leq PW50/T \leq 1.6$, where PW50 is the pulse width at the 50% amplitude point of the channel's step response and T is the duration of the channel encoded bit. A partial response maximum likelihood (PRML) system for the magnetic recording channel has been described in "A PRML system for Digital Magnetic Recording," Roy D. Cideciyan et al., IEEE Journal on Selected Areas
25 in Communications, Vol. 10, No. 1, pp. 38 - 56, January 1992. In the US patent No. 4,786,890 a class-IV PRML channel using a run-length limited (RLL) code has also been disclosed.

At high recording densities, i.e., $PW50/T > 1.6$, the linear partial-response
30 class-IV equalizer leads to substantial noise enhancement. As a consequence, the performance of the PRML detector suffers and may become inadequate to meet product specifications. Application of extended partial-response maximum likelihood (EPRML) detectors has been shown in theory and

1 practice to achieve better performance than PRML detectors in the range
PW50/T > 1.6. The patent application GB-A-2286952, published on 30 August
1995, discloses a novel EPRML scheme for data detection in a direct access
storage device. The novel architecture of the invention claimed therein allows
5 for the addition of EPRML detectors to PRML channels with only minor
changes to the overall channel architecture.

The optimum MLSD receiver for detecting an uncoded data sequence in the
presence of intersymbol-interference (ISI) and additive Gaussian noise
10 consists of a whitened-matched filter followed by a Viterbi detector which
performs maximum likelihood sequence detection on the ISI trellis, as
described by G. D. Forney in "Maximum-likelihood sequence estimation of
digital sequences in the presence of intersymbol interference," IEEE Trans.
Inform. Theory, Vol. IT-18, No. 3, pp. 363 - 378, May 1972. For the magnetic
15 recording channel the state complexity of this trellis is given by 2^L where L
represents the number of relevant ISI terms in the output signal of the
whitened-matched filter. In the patent application WO94/29989 with title
"Adaptive noise-predictive partial-response equalizing for channels with
spectral nulls," filed 14 June 1993 and published 22 December 1994, and in
20 reference "Noise predictive partial-response equalizers and applications," P.
R. Chevillat et al., IEEE Conf. Records ICC'92, June 14-18 1992, pp.
0942 - 0947, it was shown that a partial-response zero forcing equalizer
cascaded with a linear predictor whose coefficients have been suitably
chosen, is equivalent to the whitening discrete-time prefilter of the optimum
25 MLSD receiver. Furthermore, in the same patent application a receiver
structure has been disclosed where the prediction process has been
imbedded in the Viterbi detector corresponding to the partial-response trellis.
The above patent application WO94/29989 is primarily concerned with wire
transmission systems.

30 In the above patent application WO94/29989 and the article of P. R. Chevillat
et al. it has been concluded that noise-prediction in conjunction with PRML
improves detector performance.

1 It is an object of the present invention to provide a method and apparatus with improved data detection performance.

It is an object of the present invention to provide a method and apparatus for
5 improved data detection in direct access storage devices with the purpose to overcome the performance problems in prior art schemes.

It is an object of the present invention to provide a method and apparatus to achieve higher linear storage density in direct access storage devices
10 (DASDs).

It is another object of the present invention to provide a method and apparatus which can be employed in a conventional PRML/EPRML direct access storage device without changing the principal architecture of the
15 electronic channel.

SUMMARY OF THE INVENTION

20 The above objects have been accomplished by providing an entire family of estimation detectors which can for example be used for data detection in DASDs. Some of the present detectors, which make specific use of properties of the magnetic recording channel, arise by imbedding a noise prediction/whitening process into the branch metric computation of the
25 maximum-likelihood sequence detector and are collectively called Noise Predictive Maximum Likelihood (NPML) detectors. They furthermore comprise means for cancellation of intersymbol-interference (ISI) components by an appropriate table look-up. In contrast to the patent application WO94/29989 and the article of P. R. Chevillat et al. where the state complexity of the
30 detector is fixed and determined by the partial-response trellis, the NPML detectors have a state complexity which is equal to 2^K , where $0 \leq K \leq L$ and L reflects the number of controlled (known) Intersymbol Interference (ISI) components introduced by the combination of PR equalizer and predictor.

1 The special case where $K = L$ is equivalent to the optimum MLSD detector
for the given predictor length and the special case $K = 0$ corresponds to a
noise-predictive PR equalizer followed by a memoryless detector. For
• $1 \leq K < L$ the NPML detector operates on a reduced set of ISI states. At the
5 same time, the $(L-K)$ ISI terms (components) not represented in the
state-space of the NPML detector are compensated in a decision-feedback
fashion by using decisions from the path history. Thus, the NPML detectors
offer a trade-off between performance and state complexity and/or length of
decision-feedback and they provide a substantial gain in linear recording
10 density over PRML and EPRML detectors. In addition, the present
implementations of NPML detectors do not require multiplications in the
imbedded predictor and thus allow simple random access memory (RAM)
look-up implementation for ISI cancellation. Furthermore, NPML detectors
generally do not exhibit quasi-catastrophic error propagation. Thus, additional
15 increases in recording density can be achieved with higher rate run-length
limited (RLL) codes by relaxing the constraints relating to the survivor path
memory. Finally, besides modularity and substantial gains in performance, the
NPML detectors have the important implementation advantage that they can
be "piggy-backed" on existing PRML/EPRML systems. Therefore, there is no
20 need for the development and implementation of an entirely new channel
architecture which is a costly and complex task.

Also described and claimed are low complexity derivatives of the NPML
detector family which offer appreciable performance gains. The respective
25 schemes include, but are not limited to, two-state interleaved NPML detectors
and cascaded noise-predictors with PRML detectors. Furthermore, derived
from an NPML scheme with a single-tap predictor, a programmable 8-state
NPML detector is described which is capable to operate also as a PRML or
EPRML detector.

30

DESCRIPTION OF THE DRAWINGS
AND NOTATIONS USED

The invention is described in detail below with reference to the following
5 drawings:

- FIG. 1** Shows a block diagram used to illustrate how the inventive NPML detectors fit into the existing PRML channel architecture.
- 10 **FIG. 2A** Shows the blocks of Figure 1 which are relevant for the present invention: the digital equalizer 22, the present NPML detector 10, and inverse precoder 23.
- FIG. 2B** Shows an equivalent form of the present NPML detector 10,
15 according to the present invention.
- FIG. 2C** Shows another equivalent, more detailed, form of the present NPML detector 10, according to the present invention.
- 20 **FIG. 2D** Shows yet another equivalent form of the present NPML detector 10, according to the present invention.
- FIG. 2E** Shows another possible embodiment of a sequence detector with imbedded feedback, according to the present invention.
25
- FIG. 3A** Shows the noise-predictive part using a memoryless detector in cascade with a conventional PRML detector, according to the present invention.
- 30 **FIG. 3B** Shows another approach to realize the noise-predictive part using a memoryless detector in cascade with a conventional PRML detector, according to the present invention.

- 1 **FIG. 4** Shows a block diagram to illustrate the operation of the metric update unit (MUU), for some state s , at the time nT , according to the present invention. MMUs are major functional blocks in an NPML detector.
- 5 **FIG. 5** Shows a 2-state trellis diagram.
- 10 **FIG. 6** Shows an implementation of a 2-state NPML detector with a 4-tap predictor, according to the present invention.
- 15 **FIG. 7** Shows a 2-state trellis (difference metric) diagram.
- 20 **FIG. 8** Shows one possible way of mapping the algorithm implied by the trellis diagram in Figure 7 into hardware, where the threshold for the comparators is provided by the stored difference metric D_{n-1} .
- 25 **FIG. 9** Shows a 4-state trellis diagram.
- 30 **FIG. 10A-10C** Shows another implementation of an NPML detector, according to the present invention (4-state, 2-tap predictor).
- 35 **FIG. 11A-11C** Shows another implementation of an NPML detector, according to the present invention (4-state, 4-tap predictor).
- 40 **FIG. 12** Shows an 8-state trellis diagram with $N=1$ and $K=3$ (8-state, 1-tap predictor).
- 45 **FIG. 13** Shows a transformed 8-state trellis diagram with $N=1$ and $K=3$ (8-state, 1-tap predictor).

1 **FIG. 14** Shows one possible way of mapping the algorithm implied by the trellis diagram in Figure 13 into a hardware structure. The survivor path memory controlled by the select-signals S_0, \dots, S_7 , is not shown.

5 **FIG. 15** Shows an alternate form of implementing the functions of the 2-state NPML detector with a 4-tap predictor shown in Figure 6.

10 **FIG. 16A-16C** Shows another implementation of an NPML detector, according to the present invention (4-state, N-tap predictor).

15 **FIG. 17A-17C** Shows another implementation of an NPML detector, according to the present invention (4-state, N-tap predictor).

GENERAL DESCRIPTION

In the following the principal forms of implementation of NPML Detectors are described.

20 The block diagram in Figure 1 shows how the present NPML detectors 10 fit into the existing PRML channel architecture. Customer data I_n are written in the form of binary digits $a_n \in \{-1, +1\}$ by write head 15 on the disk 11 after being encoded in an encoder 12 by a rate-8/9 RLL code, serialized in a
25 serializer 13 and precoded in a precoder 14 by a $1/(1+D^2)$ operation where D is the unit delay operator. When retrieving the customer data from said disk 11, an analog signal $r(t)$ is generated by the read head 15 and provided at the read-head's output. This signal $r(t)$ is then applied via the arm electronics 16 to a variable-gain amplifier (VGA) circuit 17. The output signal of the VGA
30 circuit 17 is first low-pass filtered using an analog low-pass filter 18 (LPF) and then converted to a digital form x_n by an analog-to-digital (A/D) converter 19. The functions of the A/D converter 19 and VGA unit 17 are controlled by the timing recovery and gain control loops 20 and 21, respectively. The analog

low-pass filter 18 is preferably a filter which boosts the higher frequencies to avoid saturation of the A/D converter 19. The digital samples x_n at the output of the A/D converter 19 (line labeled A in Figure 1) are first shaped to PR4 signal samples by the digital equalizer 22 (line labeled B in Figure 1) and are then passed on to the inventive NPML detector in the form of digital samples y_n . After inverse precoding by means of a precoder 23 performing a $(1 \oplus D^2)$ operation, the output data of the NPML detector 10 (i.e. the final decisions; line labeled C in Figure 1) are fed via a deserializer 24 to a decoder 25 for the rate-8/9 RLL code which delivers the retrieved customer data \hat{I}_{n-d} . The inverse precoder function following the NPML detector in Figure 1 can be a separate functional block (as shown) or it can be imbedded in the trellis (survivor path memory) of the detector. Figure 2A shows the blocks in Figure 1 which are relevant for the present invention: the digital equalizer 22, the NPML detector 10, and the inverse precoder 23.

Generally, the coefficients of the digital equalizer 22 can be optimized so that the overall transfer function, including the head/disk-medium characteristics and the analog LPF 18, closely matches any desired system polynomial of the generalized partial-response form $f(D) = (1 + f_1 D^1 + \dots + f_p D^p)$ where the coefficients f_i can be arbitrary real numbers. For example, the partial-response (PR) polynomial for class-4 PR systems (PR4) is $f(D) = (1 - D^2)$. Similarly, the polynomial for extended partial-response class-4 (EPR4) systems is $f(D) = (1 - D^2)(1 + D) = (1 + D - D^2 - D^3)$. A further example is $f(D) = (1 - 0.1D - 0.9D^2)$.

Figure 2B shows the basic structure of the NPML detector 10 in the form of a prediction error filter 41 cascaded with a sequence detector (SD) with imbedded feedback (FB) 30.

In the sequel we use PR4- equalized signals y_n (Line B in Figure 2B), however, the inventive scheme can be applied to any shaping performed by the equalizer 22 in Figures 2A and 2B.

1 Figures 2C and 2D show two equivalent forms of NPML detectors, according
to the present invention. Its basic principle can be explained as follows. Let y_n
be the output of the PR4 digital equalizer (line labeled B in Figures 1, 2C
and 2D). This output then consists of a PR4 data signal and colored noise
5 (colored interference components), i.e.,

$$y_n = a_n - a_{n-2} + w_n \quad (1)$$

10 where $a_n \in \{-1, +1\}$ denotes the encoded/precoded data sequence written on
the magnetic medium with a rate $1/T$ and w_n represents the colored noise
sequence at the output of the digital equalizer 22. The power of the colored
noise component (colored interference component) can be reduced by noise
prediction. If $p(D) = (p_1 D^1 + p_2 D^2 + \dots + p_N D^N)$ denotes the transfer
15 polynomial, or equivalently $E(D) = 1 - P(D)$ denotes the transfer polynomial of
the prediction error filter, of the N-tap minimum mean-square (MMSE)
predictor of the noise sample w_n , then the signal

$$\begin{aligned} e_n &= w_n - \hat{w}_n = \\ 20 \quad & w_n - \sum_{i=1}^N w_{n-i} p_i = \\ & = (y_n - a_n + a_{n-2}) - \sum_{i=1}^N (y_{n-i} - a_{n-i} + a_{n-i-2}) p_i \end{aligned} \quad (2)$$

25 represents the prediction error or equivalently the whitened noise component
of the PR4-equalized output signal y_n . Reliable operation of the
prediction/whitening process is possible by using decisions from the path
history associated with each state which is available in a sequence (Viterbi)
30 detector. In that sense, NPML detectors are MLSD detectors for (PR) signals
with imbedded prediction or equivalently imbedded feedback.

In view of (1) and (2) the branch metric of the NPML detector 10 for PR4-equalized samples corresponding to a transition from state s_i to state s_k takes the form

$$\lambda(s_i, s_k) = \left| y_n - \sum_{i=1}^N (y_{n-i} - a_{n-i}(s_i) + a_{n-i-2}(s_i)) p_i - a_n + a_{n-2} \right|^2 \quad (3)$$

where the terms $a_{n-i}(s_i)$, $a_{n-i-2}(s_i)$ represent past decisions taken from the path history associated with state s_i and a_n, a_{n-2} are determined by the hypothesized state transition $s_i \rightarrow s_k$. Clearly, the noise prediction process appears explicitly in the branch metric computation of the Viterbi algorithm implementing the NPML detector. Furthermore, it can be seen that by setting the predictor coefficients p_i equal to zero, the branch metric in (3) becomes the branch metric of the 4-state PRML detector.

The branch metric in (3) can also be written as

$$\lambda(s_i, s_k) = \left| y_n - \sum_{i=1}^N y_{n-i} p_i + \sum_{i=1}^N (a_{n-i}(s_i) - a_{n-i-2}(s_i)) p_i - a_n + a_{n-2} \right|^2 \quad (4)$$

By noticing that the first sum in (4) is state independent, and after some rearrangement of the remaining terms, the equivalent branch metric is obtained as

$$\lambda(s_i, s_k) = \left| z_n + \sum_{i=K+1}^{N+2} a_{n-i}(s_j) g_i + \sum_{i=1}^K a_{n-i} g_i - a_n \right|^2 \quad (5)$$

where the signal sample $z_n = y_n - \sum_{i=1}^n y_{n-i} p_i$ is the output of the prediction error filter 41, shown in the equivalent NPML implementation of Figure 2C, and

1 { $g_i, i = 1, 2, \dots, N + 2$ } are the coefficients of the imbedded feedback filter 42 (FIR: finite impulse response or RAM-based filter) in Figure 2C. It can be shown that the coefficients { $g_i, i = 1, 2, \dots, N + 2$ } introduced in (5) are the coefficients of the polynomial

$$5 \quad g(D) = (1 - g_1 D^1 - g_2 D^2 - \dots - g_{N+2} D^{N+2}) = (1 - D^2)(1 - P(D)) = (1 - D^2)E(D).$$

The effective ISI memory L of the PR4-based NPML system is thus $L = N + 2$.

The symbols $a_{n-1}(s_i)$ in the first summation term of (5) represent past decisions taken from the path history associated with state s_i , whereas the symbols a_{n-1} in the second summation term of (5) represent state information. Clearly, by increasing K we effectively increase the number of states of the NPML detector and decrease the length of the imbedded decision feedback. Conversely, by decreasing K the number of states is decreased at the expense of increasing the length of the imbedded decision feedback. Thus, the emerging family of NPML detectors, in accordance with the present invention, offers a trade-off between state complexity and length of imbedded decision feedback.

The two equivalent implementations of the NPML detector 10 shown in Figure 2C and 2D, respectively, require no change of the signal processing blocks, i.e., VGA 17, analog LPF 18, digital equalizer 22, timing recovery and gain control loops 20 and 21, of the current PRML/EPRML channel architecture used by IBM and others. Any member of the family of NPML detectors according to the present invention can either replace the PRML/EPRML detector or operate concurrently with it.

25 A third possible implementation of an NPML scheme in the form of a filter cascaded with a sequence detector with imbedded feedback is shown in Figure 2E. In this case the combination of digital equalizer 22 and prediction error filter 41 (see Figure 2B) is replaced by a single finite-impulse response filter designated as FIR1 51. Input to the filter FIR1 51 now are the unequalized samples x_n at the output of the A/D converter 19 (line labeled A in Figure 1 and Figure 2E). The filter FIR1 51 has the property to whiten the noise and introduce a controlled amount of ISI in the signal samples z_n at its

1 output. The coefficients of the feedback filter (FIR2 or RAM 52) are then used in the branch metric computation of the sequence detector with imbedded feedback in the same way described above. Thus, the branch metric takes the form

5

$$\lambda(s_j, s_k) = \left| z_n + \sum_{i=K+1}^{N+2} a_{n-i}(s_j)b_i + \sum_{i=1}^K a_{n-i}b_i - a_n \right|^2 \quad (6)$$

10 where z_n is the output of FIR1 51 and $\{b_i, i = 1, 2, \dots, N+2\}$ is the set of coefficients of the filter FIR2 52. Note that expressions (5) and (6) are essentially the same. It can be shown that for infinitely long filters the three alternative implementations of sequence detection with imbedded feedback, shown in Figures 2A - 2E, are equivalent.

15

It should be understood that the NPML principles described hereinabove can be applied to any form of system polynomial $f(D)$. In the sequel, however, only the PR class-IV polynomial (PR4) will be considered as the target polynomial.

20

Performance and Preferred Parameters for NPML Detectors Used in DASD's:

The error performance of a magnetic recording system employing NPML detection has been studied by computer simulations in order to determine the appropriate parameters N (number of predictor coefficients) and K (length of detector memory defining the number of detector states 2^K) to be used in a practical system. In particular, the cases described in this document for $N=1$, $N=2$, and $N=4$ predictor coefficients lead to preferred NPML detectors.

25

30 Two low-complexity derivatives of the NPML detector family have also been investigated. Both schemes, like the entire family of NPML detectors, require no change of the signal processing parts of the current PRML channel architecture (see also Figure 1). Figure 3A shows the noise-predictive part using a memoryless detector in cascade with a conventional PRML detector.

1 The colored noise component of the PR4-equalized signal (line labeled B in
Figure 1 and 3A) is first whitened by a predictor. Note that instead of
imbedding the predictor into the MLSD process, a 3-level (+2, 0, -2)
memoryless detector provides the (tentative) PR4 (signal sample) decisions
5 needed for the whitening process. The PR4-equalized samples corrupted with
the whitened noise components are then fed to a conventional PRML detector
and inverse precoder to obtain improved final decisions. Figure 3B is an
equivalent form of the scheme in Figure 3A similar to the equivalent forms in
Figure 2C and 2D, respectively.

10 The second low-complexity NPML detector scheme is based on the fact that
PR4 sequences can be viewed as two independent, interleaved di-code
sequences with polynomial $(1 - D')$, where D' refers to a delay of $2T$. In this
case each di-code sequence at the output of the digital equalizer (line labeled
15 B in Figures 1, 2C, and 2D) can be described by a 2-state trellis. The Viterbi
algorithm, operating separately on each of these 2-state interleaved trellises,
will use the branch metrics given in (3) or (5) where the time indices are either
even or odd. For example, while the Viterbi algorithm operates on the even
trellis, the time indices of the branch metric expression (3) or (5) will be even
20 whereas the contribution of the odd past decisions in whitening the noise will
come from the path memory with the best metric of the odd trellis.

A further suboptimal scheme is to find the state with the best metric, compute
the predictor output using the decisions from the survivor path corresponding
25 to this best state, and applying it as a feedback term in the metric update
computations for all states. This approach has the advantage that only a
single RAM is needed.

Concept of NPML Detectors with Nonlinear Predictors:

30 The NPML concept described herein is also applicable when the noise
predictor has certain nonlinear characteristics and/or the computation of the
predictor coefficients is based on a different noise model.

- 1 The present NPML architecture allows for great flexibility in optimizing the noise predictor function with respect to various kinds of random noise which occur in a practical target system. For example, only a portion of the total noise in hard disk drives is adequately modelled by additive white Gaussian noise (AWGN). Besides AWGN, the total noise includes other noise sources, such as signal-dependent disk noise, noise due to texture scratches, and so forth. In addition, to a certain extent coherent interference, such as clock and/or adjacent track signals, may also exist in the analog readback signal.
- 10 Because the NPML concept allows, in effect, the transfer function for the signal portion of the input to be different than that for the noise and other interference components also present in the signal, the predictor may be optimized to minimize signal disturbances due to any type of corruptive source. Conventional detectors (such as PRML and EPRML detectors, etc.)
- 15 are only optimized to the extent that the signal disturbance at the detector input is additive, random, uncorrelated and Gaussian. This is often a poor approximation in practical DASD systems; thus, using a linear predictor and/or computing the predictor coefficients based on this idealistic noise model may not lead to optimal solutions in situations where this assumption is
- 20 poorly matched.

In hard disk drives, both AWGN and so-called "disk noise" are dominant sources of readback signal corruption. In the following, an example is given for a linear noise predictor with four coefficients ($N=4$) where the coefficients

25 have been computed by incorporating AWGN as well as disk noise in the noise statistics. A simple model of disk noise is the so-called "transition jitter model" wherein the deviation of each written transition from its nominal location is a random variable. The effective SNR achieved at the input of a PRML detector is 15.4dB and at the input of a 64-state NPML detector 18.9dB

30 for AWGN alone for a channel operating at $PW50/T = 3$. In case of AWGN combined with disk noise (transition jitter) the effective SNR at the input of a PRML detector is 12.7dB and at the input of a 64-state NPML detector 15.5dB for a channel operating at $PW50/T = 3$. It is interesting to note that the NPML

1 detector is able to adapt the predictor coefficients to different noise statistics
and thus to maintain an SNR margin of 2.8-3.5dB over PRML. Although this
example uses a 4-tap linear noise predictor for NPML, this technique and its
benefits is herein claimed for all possible types of noise predictors, including
5 nonlinear predictors.

Examples of Preferred Embodiments of NPML Detectors:

The preferred form of implementation of an NPML detector within a PRML
system is the one given in Figure 2C. More details on this embodiment of an
10 NPML detector 10 are given in this section. Figure 4 illustrates the operation
of a major functional block in an NPML detector according to Figure 2C - the
metric update unit (MUU) 68 shown here for state s_k at time nT . Figure 4
illustrates the required time relations between inputs and outputs of the
various functional blocks. A separate MUU function must be provided for
15 each hypothesized state s_k , $k = 1, 2, \dots, 2^K$, where $K \in \{1, 2, \dots, L\}$ and L is the
number of controlled ISI terms, e.g. for PR4 $L = N + 2$. In high-performance
DASDs parallel MUU hardware must be provided for each state to meet the
data throughput requirements; in principle, however, hardware could be
shared if speed constraints permit. Furthermore, it is assumed here and
20 hereafter that the survivor path memory (SPM) 61, as shown for example in
Figure 4, is implemented by using the register-exchange method, as for
example described in the patent application GB-A-2286952, published on 30
August 1995.

25 The branch metric (BM) units in a conventional MLSD (Viterbi) detector
require only signal sample inputs, obtained directly from the equalizer (signal
labeled B in Figure 2C). As indicated in Figure 4, it is a distinguished feature
of the NPML detectors with $K < L$ that each BM unit 62, 63 requires signal
samples processed by a predictor 41 (signal labeled z_n in Figure 2C), as well
30 as an additional input from FIR or RAM-based filters 64, 65 (signals G_s and
 G_i in Figure 4) in the feedback path between the SPM 61 and the MUU 68.
Note that the feedback filters 64, 65 do not have a common serial input, but
they are loaded in parallel at every symbol interval T . The input of each FIR

1 or RAM-based filter 64. 65 is a set of most recent past decisions taken from
the survivor path history stored in the SPM 61 for each hypothesized state
(i.e., s_i and s_j , respectively, in Figure 4). The add-compare-select (ACS) unit
66 in Figure 3 adds the branch metrics to the state metrics Ms_i and Ms_j ,
5 ~~respectively~~, respectively, compares the results, selects the survivor metric Ms_k and
provides the update signal Ss_k for the corresponding decision path in the SPM
61. The SPM 61 produces final decisions at output line 67 with a delay of dT
seconds relative to time nT . It is a further feature of the present NPML
10 detector that the delay parameter d can generally be made shorter compared
to that of a conventional MLSD detector designed for PR signaling (i.e., PR
signaling schemes with spectral nulls, such as PR4).

**NPML Detector Using Four Predictor Coefficients
(N=4) and Two States (K=1):**

15 For $N=4$ and $K=1$ the branch metrics based on (5) become

$$20 \quad \lambda(s_j, s_k) = \left| z_n + \sum_{i=2}^6 a_{n-i}(s_j)g_i + a_{n-1}g_1 - a_n \right|^2 \quad (7)$$

where the signal sample $z_n = y_n - \sum_{i=1}^4 y_{n-i}p_i$ is the output of the prediction
error filter 41. Associating the data symbols "+1" and "-1" with the binary
numbers 1 and 0, respectively, the state information $a_{n-1} = +1(-1)$ is
25 mapped into the present state $s_i = 1(0)$ and the present data symbol
 $a_n = +1(-1)$ mapped into the next state $s_j = 1(0)$. Letting

$$30 \quad G1_{n-1} = \sum_{i=2}^6 a_{n-i}(1)g_i \quad (8)$$

$$G0_{n-1} = \sum_{i=2}^6 a_{n-i}(0)g_i \quad (9)$$

one obtains the four branch metrics

$$\lambda(1,1) = |z_n + G1_{n-1} + g_1 - 1|^2 \quad (10)$$

$$\lambda(1,0) = |z_n + G1_{n-1} + g_1 + 1|^2 \quad (11)$$

$$\lambda(0,1) = |z_n + G0_{n-1} - g_1 - 1|^2 \quad (12)$$

$$\lambda(0,0) = |z_n + G0_{n-1} - g_1 + 1|^2 \quad (13)$$

where z_n are the samples obtained from the corresponding 4-tap prediction error filter connected in cascade with the equalizer (see Figure 2C). It will be useful to define the quantities

$$Z11_n = z_n + g_1 - 1 \quad (14)$$

$$Z10_n = z_n + g_1 + 1 \quad (15)$$

$$Z01_n = z_n - g_1 - 1 \quad (16)$$

$$Z00_n = z_n - g_1 + 1 \quad (17)$$

since they can be precomputed outside the feedback loop, if necessary by means of pipelining. Thus, eqs. (10) - (13) can be written as

$$\lambda(1.1) = |Z11_n + G1_{n-1}|^2 \quad (18)$$

$$\lambda(1.0) = |Z10_n + G1_{n-1}|^2 \quad (19)$$

$$\lambda(0.1) = |Z01_n + G0_{n-1}|^2 \quad (20)$$

$$\lambda(0.0) = |Z00_n + G0_{n-1}|^2 \quad (21)$$

respectively. Finally, defining the stored metrics $M1_n$ and $M0_n$ for states 1 and 0, respectively, the trellis diagram shown in Figure 5 is obtained. The metrics are updated according to

$$M1_n = \min \{M1_{n-1} + \lambda(1.1); M0_{n-1} + \lambda(0.1)\} \quad (22)$$

$$M0_n = \min \{M1_{n-1} + \lambda(1.0); M0_{n-1} + \lambda(0.0)\} \quad (23)$$

and direct mapping of the trellis shown in Figure 5 into hardware functions leads to the implementation of the 2-state NPML detector with a 4-tap predictor 77 shown in Figure 6. It is proposed here to generate the terms $G1_{n-1}$ and $G0_{n-1}$, defined by (8) and (9), respectively, by means of RAM-based filter structures 71, 72 which can be loaded with the appropriate (five) path history decisions. Also indicated in Figure 6 is the 2-state SPM 70 fed by the two comparators 58. In an alternate embodiment (not shown), the functions of SPM 70 and RAM-based filters 71, 72 shown in Figure 6 could be combined in an attempt to speed-up computation of $G1_n$ and $G0_n$. Note further, that the squaring functions in Figure 6, realized by means of units 73-76, can be approximated to simplify the required circuitry, with minimal loss in performance. The decision signals S1 and S0 in Figure 6 are used to control

1 the metric multiplexers 79 and the path update in the SPM 70. The selected
metrics $M1_n$ and $M0_n$ are stored in registers 80 and 81, respectively.

A multitude of variations of the implementation shown in Figure 6 is possible,
5 depending on constraints, complexity, critical timing paths, and algorithmic
issues such as metric bounding. For example, automatic metric bounding can
be achieved by using the conventional modulo technique in the adders 82-85
feeding the comparator inputs 58, as described in "An Alternative to metric
rescaling in Viterbi decoders," A.P. Hekstra, IEEE Transactions on
10 Communications, Vol. 37, No. 11, pp. 1220-1222, November 1989. An
alternate method of metric normalization can be implemented by applying the
concept of a difference metric. Defining the difference metric

$$15 \quad D_{n-1} = M1_{n-1} - M0_{n-1} \quad (24)$$

the trellis in Figure 7 is obtained where the metrics are updated such that the
metric for state 0 is always the zero-valued metric. Thus, the difference metric
is updated according to

$$20 \quad D_n = \min \{D_{n-1} + \lambda(1,1); \lambda(0,1)\} - \min \{D_{n-1} + \lambda(1,0); \lambda(0,0)\} \quad (25)$$

where one can show that the cross-extension of the trellis in Figure 7, which
would lead to the difference metric $D_n = \lambda(0,1) - [D_{n-1} + \lambda(1,0)]$, is not
25 possible. Thus, only three of the four potential values of D_n in (25) will have to
be considered. One possible way of mapping the algorithm implied by the
trellis description in Figure 7 into hardware is shown in Figure 8 where the
threshold for the comparators is now provided by the difference metric D_{n-1}
stored in register 80. Figure 8 is otherwise similar to Figure 6. The
30 difference metric approach is useful in cases where it is not possible or
convenient to use the conventional modulo technique which relies on
2s-complement arithmetic for metric normalization.

1 **NPML Detector Using Two Predictor Coefficients**
(N = 2) and Four States (K = 2):

For N=2 and K=2, i.e., $2^K = 4$ states, the branch metrics based on (5) become

$$\lambda(s_j, s_k) = \left| z_n + \sum_{i=3}^4 a_{n-i}(s_j)g_i + a_{n-1}g_1 + a_{n-2}g_2 - a_n \right|^2 \quad (26)$$

10 where the signal sample $z_n = y_n - y_{n-1}p_1 - y_{n-2}p_2$ is the output of the 2-tap prediction error filter. Associating again the data symbols "+1" and "-1" with the binary numbers 1 and 0, respectively, we map the state information $(a_{n-2}, a_{n-1}) = (-1, -1), (-1, +1), (+1, -1)$ and $(+1, +1)$ into the present state $s_j = 0, 1, 2,$ and $3,$ respectively. Similarly, the next state information
 15 $(a_{n-1}, a_n) = (-1, -1), (-1, +1), (+1, -1)$ and $(+1, +1)$ is mapped into the next state $s_k = 0, 1, 2,$ and $3,$ respectively. Letting

$$20 \quad G3_{n-1} = \sum_{i=3}^4 a_{n-i}(3)g_i = a_{n-3}(3)g_3 + a_{n-4}(3)g_4, \quad (27)$$

$$25 \quad G2_{n-1} = \sum_{i=3}^4 a_{n-i}(2)g_i = a_{n-3}(2)g_3 + a_{n-4}(2)g_4, \quad (28)$$

$$30 \quad G1_{n-1} = \sum_{i=3}^4 a_{n-i}(1)g_i = a_{n-3}(1)g_3 + a_{n-4}(1)g_4, \quad (29)$$

$$G0_{n-1} = \sum_{i=3}^4 a_{n-i}(0)g_i = a_{n-3}(0)g_3 + a_{n-4}(0)g_4, \quad (30)$$

one obtains the eight branch metrics

$$\lambda(3,3) = |z_n + G3_{n-1} + g_1 + g_2 - 1|^2 \quad (31)$$

$$\lambda(3,2) = |z_n + G3_{n-1} + g_1 + g_2 + 1|^2 \quad (32)$$

$$\lambda(2,1) = |z_n + G2_{n-1} + g_1 - g_2 - 1|^2 \quad (33)$$

$$\lambda(2,0) = |z_n + G2_{n-1} + g_1 - g_2 + 1|^2 \quad (34)$$

$$\lambda(1,3) = |z_n + G1_{n-1} - g_1 + g_2 - 1|^2 \quad (35)$$

$$\lambda(1,2) = |z_n + G1_{n-1} - g_1 + g_2 + 1|^2 \quad (36)$$

$$\lambda(0,1) = |z_n + G0_{n-1} - g_1 - g_2 - 1|^2 \quad (37)$$

$$\lambda(0,0) = |z_n + G0_{n-1} - g_1 - g_2 + 1|^2 \quad (38)$$

where z_n are the samples obtained from the corresponding 2-tap predictor filter connected in cascade with the equalizer, see Figure 2C. It will be useful to define the quantities

$$Z33_n = z_n + g_1 + g_2 - 1 \quad (39)$$

$$Z32_n = z_n + g_1 + g_2 + 1 \quad (40)$$

$$Z21_n = z_n + g_1 - g_2 - 1 \quad (41)$$

$$Z20_n = z_n + g_1 - g_2 + 1 \quad (42)$$

$$Z13_n = z_n - g_1 + g_2 - 1 \quad (43)$$

$$Z12_n = z_n - g_1 + g_2 + 1 \quad (44)$$

$$Z01_n = z_n - g_1 - g_2 - 1 \quad (45)$$

$$Z00_n = z_n - g_1 - g_2 + 1 \quad (46)$$

since they can be precomputed outside the feedback loop, if necessary by means of pipelining. Thus, eqs. (31) - (38) can be written as

$$\lambda(3,3) = |Z33_n + G3_{n-1}|^2 \quad (47)$$

$$\lambda(3,2) = |Z32_n + G3_{n-1}|^2 \quad (48)$$

$$\lambda(2,1) = |Z21_n + G2_{n-1}|^2 \quad (49)$$

$$\lambda(2,0) = |Z20_n + G2_{n-1}|^2 \quad (50)$$

$$\lambda(1,3) = |Z13_n + G1_{n-1}|^2 \quad (51)$$

$$\lambda(1.2) = |Z12_n + G1_{n-1}|^2, \quad (52)$$

$$\lambda(0.1) = |Z01_n + G0_{n-1}|^2, \quad (53)$$

$$\lambda(0.0) = |Z00_n + G0_{n-1}|^2, \quad (54)$$

respectively. Finally, defining the stored (present) metrics $Ms_{i_{n-1}}$ for each of the present states $s_i = 0, 1, 2$, and 3, one obtains the trellis diagram shown in Figure 9. The four metrics for the next states $s_k = 0, 1, 2$, and 3, are updated according to

$$Ms_{k_n} = \min \{Ms_{i_{n-1}} + \lambda(s_i, s_k); Ms_{j_{n-1}} + \lambda(s_j, s_k)\}, \quad (55)$$

with s_i and s_j being the possible present states. Direct mapping of the trellis shown in Figure 9 into hardware functions leads to the scheme shown in Figures 10A, 10B, 10C. The terms $G0_{n-1}$, $G1_{n-1}$, $G2_{n-1}$, and $G3_{n-1}$, defined by (27) - (30), respectively, can be generated by means of a random access memory 131-134 (RAM) which stores the appropriate values for the given coefficient g_1 and g_2 , depending on the chosen operating point of the channel; the RAMs 131-134 need to hold only four different (actually two different and their negative) values. The 4-state SPM 135 is a register-exchange structure in case of high-speed implementation. Note that the squaring functions in (31) - (38) can be approximated to simplify the required circuitry, with minimal loss in performance. Four decision signals ($S0$, $S1$, $S2$, $S3$) are needed to control the metric multiplexers and the path update in the SPM 135. Automatic metric bounding is achieved by using the conventional modulo-2 technique in the adders 136-143 feeding the comparator inputs.

**NPML Detector Using Four Predictor Coefficients (N=4)
and Four States (K=2):**

For N=4 and K=2, i.e., $2^K = 4$ states, the branch metrics based on (5) become

$$\lambda(s_j, s_k) = \left| z_n + \sum_{i=3}^6 a_{n-i}(s_j)g_i + a_{n-1}g_1 + a_{n-2}g_2 - a_n \right|^2 \quad (56)$$

where the signal sample $z_n = y_n - \sum_{i=1}^4 y_{n-i}p_i$ is the output of the prediction error filter. Associating again the data symbols "+1" and "-1" with the binary numbers 1 and 0, respectively, the state information $(a_{n-2}, a_{n-1}) = (-1, -1), (-1, +1), (+1, -1)$, and $(+1, +1)$, is mapped into the present state $s_i = 0, 1, 2$, and 3, respectively. Similarly, the next state information $(a_{n-1}, a_n) = (-1, -1), (-1, +1), (+1, -1)$, and $(+1, +1)$, is mapped into the next state $s_k = 0, 1, 2$, and 3, respectively. Letting

$$G3_{n-1} = \sum_{i=3}^6 a_{n-i}(3)g_i \quad (57)$$

$$G2_{n-1} = \sum_{i=3}^6 a_{n-i}(2)g_i \quad (58)$$

$$G1_{n-1} = \sum_{i=3}^6 a_{n-i}(1)g_i \quad (59)$$

$$G0_{n-1} = \sum_{i=3}^6 a_{n-i}(0)g_i \quad (60)$$

1 one obtains the eight branch metrics

$$\lambda(3,3) = |z_n + G3_{n-1} + g_1 + g_2 - 1|^2 \quad (61)$$

5

$$\lambda(3,2) = |z_n + G3_{n-1} + g_1 + g_2 + 1|^2 \quad (62)$$

10

$$\lambda(2,1) = |z_n + G2_{n-1} + g_1 - g_2 - 1|^2 \quad (63)$$

$$\lambda(2,0) = |z_n + G2_{n-1} + g_1 - g_2 + 1|^2 \quad (64)$$

15

$$\lambda(1,3) = |z_n + G1_{n-1} - g_1 + g_2 - 1|^2 \quad (65)$$

$$\lambda(1,2) = |z_n + G1_{n-1} - g_1 + g_2 + 1|^2 \quad (66)$$

20

$$\lambda(0,1) = |z_n + G0_{n-1} - g_1 - g_2 - 1|^2 \quad (67)$$

$$\lambda(0,0) = |z_n + G0_{n-1} - g_1 - g_2 + 1|^2 \quad (68)$$

25 where z_n are the samples obtained from the corresponding 4-tap prediction error filter connected in cascade with the equalizer (see Figure 2C). It is useful to define the quantities

30

$$Z33_n = z_n + g_1 + g_2 - 1 \quad (69)$$

$$Z32_n = z_n + g_1 + g_2 + 1 \quad (70)$$

$$Z21_n = z_n + g_1 - g_2 - 1 \quad (71)$$

$$Z20_n = z_n + g_1 - g_2 + 1 \quad (72)$$

$$Z13_n = z_n - g_1 + g_2 - 1 \quad (73)$$

$$Z12_n = z_n - g_1 + g_2 + 1 \quad (74)$$

$$Z01_n = z_n - g_1 - g_2 - 1 \quad (75)$$

$$Z00_n = z_n - g_1 - g_2 + 1 \quad (76)$$

since they can be precomputed outside the feedback loop, if necessary by means of pipelining. Thus, eqs. (61) - (68) can be written as

$$\lambda(3.3) = |Z33_n + G3_{n-1}|^2 \quad (77)$$

$$\lambda(3.2) = |Z32_n + G3_{n-1}|^2 \quad (78)$$

$$\lambda(2.1) = |Z21_n + G2_{n-1}|^2 \quad (79)$$

$$\lambda(2.0) = |Z20_n + G2_{n-1}|^2 \quad (80)$$

$$\lambda(1.3) = |Z13_n + G1_{n-1}|^2 \quad (81)$$

$$\lambda(1,2) = |Z12_n + G1_{n-1}|^2, \quad (82)$$

$$\lambda(0,1) = |Z01_n + G0_{n-1}|^2, \quad (83)$$

$$\lambda(0,0) = |Z00_n + G0_{n-1}|^2, \quad (84)$$

respectively. Finally, defining the stored (present) metrics $Ms_{i_{n-1}}$ for each of the present states $s_i = 0, 1, 2$, and 3, one obtains the trellis diagram shown in Figure 9. The four metrics for the next states $s_i = 0, 1, 2$, and 3, are updated according to

$$Ms_{k_n} = \min \{ Ms_{i_{n-1}} + \lambda(s_j, s_k); Ms_{i_{n-1}} + \lambda(s_i, s_k) \}, \quad (85)$$

with s_i and s_j being the possible present states. Direct mapping of the trellis shown in Figure 9 into hardware functions leads to an implementation structure shown in Figures 11A, 11B, and 11C. Note the similarity, respectively the differences, compared to Figures 10A, 10B, 10C (size of predictor filter and RAM address length). The terms $G0_{n-1}$, $G1_{n-1}$, $G2_{n-1}$, and $G3_{n-1}$, defined by (57) - (60), respectively, can be generated by means of RAM structures which can be loaded with appropriate values depending on the chosen operating point of the channel: the 4-state SPM can again be a register-exchange structure. Note that the squaring functions in (61) - (68) can be approximated to simplify the required circuitry, with minimal loss in performance. Four decision signals $S0$, $S1$, $S2$, and $S3$, are needed to control the metric multiplexers and the path update in the SPM.

A multitude of variations for the implementation of the 4-state NPML detector with a 4-tap noise predictor is possible, depending on constraints on complexity, critical timing paths, and algorithmic issues such as metric bounding. For example, automatic metric bounding can be achieved by using

1 the conventional modulo technique in the adders feeding the comparator
inputs. The alternate method of metric normalization, the difference metric
technique introduced above, can be extended to the 4-state NPML detector,
for example, by updating the metrics such that the stored metric of state 0 is
5 always the zero-valued metric. Further variations for implementing (4-state)
NPML detectors can be obtained by explicit expansion of the squaring
function involved in evaluating the branch metrics $\lambda(s_i, s_v)$.

NPML Detector Using a Single-Tap Predictor (N=1)

10 and Eight States (K=N+2=3):

It was pointed out hereinbefore that the 8-state NPML detector which uses a
single-tap predictor (i.e., the case where N=1 and K=N+2=3 so that $2^K = 8$
states) is a member within the family of NPML detectors which is of specific
15 practical interest for DASD applications. Since in this particular case there is
no feedback based on past decisions, i.e., the detector uses only
(hypothesized) state information for noise prediction, the feedback loops via
the FIR or RAM-based filters 64 and 65, as shown in Figure 4, are not present.
For N=1 and K=3 the 16 branch metrics based on (5) become

$$20 \quad \lambda(s_j, s_k) = |z_n + a_{n-1}g_1 + a_{n-2}g_2 + a_{n-3}g_3 - a_n|^2 \quad (86)$$

where the signal sample $z_n = y_n - p_1 y_{n-1}$. Furthermore, since in (86)
25 $g_1 = p_1$, $g_2 = 1$, and $g_3 = -p_1$, we can write

$$30 \quad \lambda(s_j, s_k) = |z_n + a_{n-1}p_1 + a_{n-2} - a_{n-3}p_1 - a_n|^2 \quad (87)$$

where the triple $(a_{n-3}, a_{n-2}, a_{n-1})$ represents the hypothesized state s_i , a_n is the
hypothesized transmitted symbol, and the triple (a_{n-2}, a_{n-1}, a_n) represents the
30 resulting next state s_v . In this situation it is advantageous to evaluate the
square on the right hand side of (87), to drop all state-independent terms, and

1 to scale the remaining expression. In this way, one arrives at the equivalent
branch metric

$$\begin{aligned}
 \lambda'(s_j, s_k) = & -[a_n - a_{n-2} - (a_{n-1} - a_{n-3})p_1]z_n \\
 & - (a_n a_{n-1} + a_{n-2} a_{n-3})p_1 - a_n a_{n-2} \\
 & + (a_n a_{n-3} + a_{n-1} a_{n-2})p_1 - a_{n-1} a_{n-3} p_1^2.
 \end{aligned} \tag{88}$$

We now arbitrarily use a somewhat different rule than the one used above to
10 map the state information into the corresponding state number, namely,
 $s_i = (a_{n-3}, a_{n-2}, a_{n-1}) = (-1, -1, -1)$ maps to the state 0,
 $s_i = (a_{n-3}, a_{n-2}, a_{n-1}) = (+1, -1, -1)$ maps to the state 1, ...
 $s_j = (a_{n-3}, a_{n-2}, a_{n-1}) = (+1, +1, +1)$ maps to state 7. Next, adding the
state-independent term $(1 + p^2)$ to all sixteen branch metrics represented by
15 (88) and dividing the result by 2, the equivalent branch metrics can be listed
as

$$\lambda''(0,0) = \lambda''(2,5) = \lambda''(5,2) = \lambda''(7,7) = 0 \tag{89}$$

20

$$\lambda''(0,4) = \lambda''(5,6) = -z_n + 1 \tag{90}$$

$$\lambda''(1,0) = \lambda''(3,5) = p_1(-z_n + p_1) \tag{91}$$

25

$$\lambda''(1,4) = \alpha(-z_n + \alpha) \tag{92}$$

$$\lambda''(2,1) = \lambda''(7,3) = z_n + 1 \tag{93}$$

30

$$\lambda''(3,1) = \beta(z_n + \beta) \tag{94}$$

$$\lambda''(4,2) = \lambda''(6,7) = p_1(z_n + p_1) \quad (95)$$

$$\lambda''(4,6) = \beta(-z_n + \beta) \quad (96)$$

$$\lambda''(6,3) = \alpha(z_n + \alpha) \quad (97)$$

where

$$\alpha = 1 + p_1, \quad \beta = 2 - \alpha = 1 - p_1, \quad z_n = y_n - p_1 y_{n-1} \quad (98)$$

Defining the stored metrics $Ms_{i,n-1}$ for the states $s_i = 0, 1, \dots, 7$, one arrives at the trellis diagram shown in Figure 12. The eight metrics $Ms_{i,n}$ for the next states $s_i = 0, 1, \dots, 7$, are updated according to

$$Ms_{k,n} = \min \{ Ms_{j,n-1} + \lambda''(s_j, s_k); Ms_{i,n-1} + \lambda''(s_i, s_k) \} \quad (99)$$

with s_j and s_i being the states at time $n-1$, according to the trellis in Figure 12. The latter can in principle be mapped directly into a hardware structure.

The trellis in Figure 12 can be further simplified by applying a similar transformation technique as described in the patent application GB-A-2286952, published on 30 August 1995; the resulting transformed trellis is shown in Figure 13 where 12 of the 16 branch metrics are zero-valued and the remaining four have values $2p_1$ or $-2p_1$. Defining the filtered samples

$$Y_n = -p_1 y_{n+1} + (1 + p_1^2) y_n - p_1 y_{n-1} \quad (100)$$

where $y_n = a_n - a_{n-2} + \text{noise}$ is the PR4-equalized, noisy sample, the quantities Z_n and Q_n shown in the trellis of Figure 13 can be expressed as

$$Z_n = Y_n + (1 + p_1^2) \quad (101)$$

and

$$Q_n = -Y_n + (1 + p_1^2) = -Z_n + 2(1 + p_1^2) \quad (102)$$

respectively; if necessary, these quantities can be computed by pipelined circuitry since they are not part of the metric feedback loop. Direct mapping of the trellis in Figure 13 into a hardware structure leads to the scheme shown in Figure 14; the eight decision signals $S_0 - S_7$ also control the operation of an 8-state SPM (register-exchange) not specifically shown. The SPM delivers the final decisions via the inverse precoder.

A significant feature of the NPML scheme described by Figures 12 - 14 is its ability to perform the detection function for arbitrary values of the noise predictor coefficient p_1 . Thus, by programming the hardware with the best suited predictor coefficient (depending on the channel operating point), optimal detection is obtained within the constraints of a single-tap predictor. In particular, by setting $p_1 = 0$, the scheme performs detection for PR4 signals, i.e., the hardware operates as a PRML detector. On the other hand, setting $p_1 = -1$, the scheme performs detection for EPR4 signals, i.e., the hardware operates as an EPRML detector. The maximum required length of the SPM or, equivalently, the maximum decision delay for the final decisions, should be chosen such that the performance can be maintained for the most sensitive scheme (e.g. EPRML).

For implementation purposes, it may be advantageous to modify the algorithm outlined for the flexible 8-state, single-tap predictor NPML scheme by adding a convenient, state-independent term to Z_n defined in eq. (101), e.g., such that $Z_n \rightarrow Z'_n = Y_n$. It has been shown in the patent application GB-A-2286952, published on 30 August 1995, that the performance of the EPRML is not affected by such a measure since the channel is DC-free (spectral null at zero

frequency); this property extends to NPML detectors as well. Thus, an alternate version of the scheme in Figure 14 is obtained by modifying Z_n and Q_n such that $Z_n \rightarrow Z'_n = Y_n$ and $Q_n \rightarrow Q'_n = -Y_n + 2(1 + p_1^2) = -Z'_n + 2(1 + p_1^2)$, respectively. Note that the condition $Z_n + Q_n = Z'_n + Q'_n = 2(1 + p_1^2)$, must always be satisfied by theory. However, as described in the patent application GB-A-2286952, published on 30 August 1995, it may be advantageous in practice to modify this condition such that $Z_n + Q_n = Z'_n + Q'_n = 2(1 + p_1^2) - \gamma$, where γ is a small, positive constant; a practical value may be $\gamma = 0.25$.

Alternate Forms of Implementation and Modifications:

This section further demonstrates the multitude of forms of implementation which are possible for NPML detectors according to the present invention. Some alternate forms and simplifications of the detectors presented above are now described in some detail:

2-State, 4-Tap Predictor NPML:

Letting

$$G1'_{n-1} = g_1 + \sum_{i=2}^6 a_{n-i}(1)g_i \quad (103)$$

$$G0'_{n-1} = -g_1 + \sum_{i=2}^6 a_{n-i}(0)g_i \quad (104)$$

one obtains the four equivalent branch metrics

$$\lambda(1,1) = |z_n + G1'_{n-1} - 1|^2 \quad (105)$$

$$\lambda(1,0) = |z_n + G1'_{n-1} + 1|^2 \quad (106)$$

$$\lambda(0,1) = |z_n + G0'_{n-1} - 1|^2 \quad (107)$$

$$\lambda(0,0) = |z_n + G0'_{n-1} + 1|^2 \quad (108)$$

where z_n are the samples obtained from the corresponding 4-tap prediction error filter connected in cascade with the equalizer (see Figure 2C). It is useful to define the new quantities

$$Z1_n = z_n - 1 \quad (109)$$

$$Z0_n = z_n + 1 \quad (110)$$

so that eqs. (105) - (108) can be written as

$$\lambda(1,1) = |Z1_n + G1'_{n-1}|^2 \quad (111)$$

$$\lambda(1,0) = |Z0_n + G1'_{n-1}|^2 \quad (112)$$

$$\lambda(0,1) = |Z1_n + G0'_{n-1}|^2 \quad (113)$$

$$\lambda(0,0) = |Z0_n + G0'_{n-1}|^2 \quad (114)$$

The alternate form of implementing the functions of Figure 6 is shown in Figure 15. Here, it is proposed to generate the terms $G1'_{n-1}$ and $G0'_{n-1}$, defined by (103) and (104), respectively, by means of random access memory

table look-up where the RAMs 121, 122 can be loaded with appropriate values (32 for each RAM) depending on the chosen operating point of the channel. The SPM 123 provides the five address bits $a_{n-2}(1), \dots, a_{n-6}(1)$ and $a_{n-2}(0), \dots, a_{n-6}(0)$ for the RAMs 121 and 122, respectively, as indicated in Figure 15.

Computation of the branch metrics for the difference metric approach (Figure 8) can be modified similarly; in this case, further simplifications are possible. For example, the potential difference metrics $D_n = \lambda(0,1) - \lambda(0,0) = -4(z_n + G0'_{n-1})$ and $D_n = \lambda(1,1) - \lambda(1,0) = -4(z_n + G1'_{n-1})$ which have to be precomputed, have simple expressions in terms of the signal sample z_n and the respective quantities generated by the RAMs.

15 -4-State, N-Tap Predictor NPML where $N=2$ or 4 (Alternative 1):

Letting

$$20 \quad G3'_{n-1} = g_1 + g_2 + \sum_{i=3}^{N+2} a_{n-i}(3)g_i \quad (115)$$

$$25 \quad G2'_{n-1} = g_1 - g_2 + \sum_{i=3}^{N+2} a_{n-i}(2)g_i \quad (116)$$

$$30 \quad G1'_{n-1} = -g_1 + g_2 + \sum_{i=3}^{N+2} a_{n-i}(1)g_i \quad (117)$$

$$G0'_{n-1} = -g_1 - g_2 + \sum_{i=3}^{N+2} a_{n-i}(0)g_i \quad (118)$$

one obtains the eight equivalent branch metrics

$$\lambda(3,3) = |z_n + G3'_{n-1} - 1|^2 \quad (119)$$

$$\lambda(3,2) = |z_n + G3'_{n-1} + 1|^2 \quad (120)$$

$$\lambda(2,1) = |z_n + G2'_{n-1} - 1|^2 \quad (121)$$

$$\lambda(2,0) = |z_n + G2'_{n-1} + 1|^2 \quad (122)$$

$$\lambda(1,3) = |z_n + G1'_{n-1} - 1|^2 \quad (123)$$

$$\lambda(1,2) = |z_n + G1'_{n-1} + 1|^2 \quad (124)$$

$$\lambda(0,1) = |z_n + G0'_{n-1} - 1|^2 \quad (125)$$

$$\lambda(0,0) = |z_n + G0'_{n-1} + 1|^2 \quad (126)$$

where z_n are the samples obtained from the corresponding N-tap prediction error filter connected in cascade with the equalizer (see Figure 2C). By making use of the definitions $Z1_n = z_n - 1$ and $Z0_n = z_n + 1$, respectively, eqs. (119) - (126) can be written as

$$\lambda(3,3) = |Z1_n + G3'_{n-1}|^2 \quad (127)$$

$$\lambda(3,2) = |Z0_n + G3'_{n-1}|^2 \quad (128)$$

$$\lambda(2,1) = |Z1_n + G2'_{n-1}|^2 \quad (129)$$

$$\lambda(2,0) = |Z0_n + G2'_{n-1}|^2 \quad (130)$$

$$\lambda(1,3) = |Z1_n + G1'_{n-1}|^2 \quad (131)$$

$$\lambda(1,2) = |Z0_n + G1'_{n-1}|^2 \quad (132)$$

$$\lambda(0,1) = |Z1_n + G0'_{n-1}|^2 \quad (133)$$

$$\lambda(0,0) = |Z0_n + G0'_{n-1}|^2 \quad (134)$$

respectively, yielding again the trellis diagram shown in Figure 9. Direct mapping of this trellis into hardware functions - by using the new variables as defined above - leads to the structure shown in Figures 16A, 16B, 16C. The terms $G0'_n$, $G1'_n$, $G2'_n$, and $G3'_n$, defined by (115) - (118), respectively, can again be generated by means of RAMs 151-154 which can be loaded with the appropriate values depending on the chosen operating point of the channel: the 4-state SPM 155 - assuming again a register-exchange structure - provides the N address bits for each of the four RAMs (one per state); equivalently, these four RAMs 151-154 can be combined into a single RAM structure with multiple inputs and outputs. Automatic metric bounding is achieved by using the conventional modulo-2 technique in the adders feeding the comparator inputs.

NPML Detectors Implemented by Analog VLSI Technology:

Implementation of any detector included within the family of NPML detectors can be done in either digital, analog, or mixed digital/analog VLSI circuit technology. Implementations in analog technology are of particular interest in.

- 1 high data rate and/or low-power applications. An example for PRML is described in "Analog Implementation of Class-IV Partial-Response Viterbi Detector", A.H. Shakiba et al., Proc. ISCAS'94, 1994; similar methods can be applied to NPML detectors.

5

NPML Detectors with Reduced SPM Length:

- It was indicated above, that NPML detectors generally do not exhibit quasi-catastrophic error propagation. This property can be exploited to save hardware and reduce decoding delay by reducing the length of the path memory in the Viterbi detector without compromising performance. On the other, these hardware savings may be traded for additional increases in recording density by using run-length limited (RLL) codes with a higher rate than 8/9, since the code constraints relating to the length of the SPM can be relaxed.

15

4-State, N-Tap Predictor NPML where N=2 or 4 (Alternative 2):

Letting in (119) - (126)

20

$$G33'_{n-1} = G3'_{n-1} - 1 \quad (135)$$

$$G32'_{n-1} = G3'_{n-1} + 1 \quad (136)$$

25

and so on, we can write the eight branch metrics as

$$\lambda(3.3) = |z_n + G33'_{n-1}|^2 \quad (137)$$

30

$$\lambda(3.2) = |z_n + G32'_{n-1}|^2 \quad (138)$$

$$\lambda(2.1) = |z_n + G21'_{n-1}|^2 \quad (139)$$

$$\lambda(2,0) = |z_n + G20'_{n-1}|^2 \quad (140)$$

$$\lambda(1,3) = |z_n + G13'_{n-1}|^2 \quad (141)$$

$$\lambda(1,2) = |z_n + G12'_{n-1}|^2 \quad (142)$$

$$\lambda(0,1) = |z_n + G01'_{n-1}|^2 \quad (143)$$

$$\lambda(0,0) = |z_n + G00'_{n-1}|^2 \quad (144)$$

15 This version leads to the implementation shown in Figures 17A, 17B, 17C where the squaring function can be approximated as shown by A. Eshraghi et al., in "Design of a New Squaring Function for the Viterbi Algorithm", IEEE Journal of Solid State Circuits, Vol. 29, No. 9, September 1994, pp. 1102 - 1107.

CLAIMS

1. Apparatus for noise predictive maximum likelihood (NPML) sequence detection in a channel, comprising:
- 5 a) a prediction error filter for whitening colored random noise components of a sample y_n received via said channel, said sample y_n comprising a generalized partial-response signal component corrupted by said colored random noise components, leading to a signal z_n now having L intersymbol-interference components,
 - 10 b) a sequence detector having
 - a state complexity being equal to 2^K , with $0 \leq K \leq L$ and L reflecting the number of said intersymbol interference components, and
 - survivor path means for storing path history decisions corresponding to 2^K survivor paths.
 - 15 c) means for cancellation of $L-K$ of said L intersymbol-interference components, said means comprising
 - feedback means for intersymbol-interference cancellation using precomputed and stored intersymbol-interference cancellation terms, and
 - 20 • means for retrieving said intersymbol-interference cancellation terms by applying said path history decisions as addresses to said feedback means for intersymbol-interference cancellation.
 - 25
2. The apparatus of claim 1, wherein said means for cancellation comprises at least one random access memory for storing said intersymbol interference cancellation terms, said random access memory being arranged such that intersymbol-interference cancellation terms are
- 30 retrieved by applying a path history decision taken from said survivor path means as address to said random access memory.

- 1 3. The apparatus of claim 1, wherein said sample y_n received via said
channel is a partial-response signal and in particular a partial-response
class-4 (PR4) shaped signal.
- 5 4. The apparatus of claim 1, wherein said sequence detector is a Viterbi
detector.
- 10 5. The apparatus of claim 1, wherein said sequence detector is a 2-state
sequence detector and said prediction error filter comprising a 4-tap
predictor.
- 15 6. The apparatus of claim 1, wherein said sequence detector is a 4-state
sequence detector and said prediction error filter comprising a 2-tap
predictor.
- 20 7. The apparatus of claim 1, wherein said sequence detector is a 4-state
sequence detector and said prediction error filter comprising a 4-tap
predictor.
- 25 8. The apparatus of claim 1, wherein said sequence detector is a 8-state
sequence detector, preferably a programmable one, and said prediction
error filter comprising a 1-tap predictor.
- 30 9. The apparatus of claim 1, either comprising a separate inverse precoder
fed by the output of said detector, or means for imbedding the inverse
precoder function into said sequence detector.
10. The apparatus of claim 1, having a transfer function for the signal portion
of said sample y_n being different from the transfer function for said
colored random noise components.

- 1 11. The apparatus of claim 2, wherein said prediction error filter and/or said
random access memory has a non-linear transfer characteristic.
12. The apparatus of claim 2, wherein said prediction error filter and/or said
5 random access memory is programmable.
13. The apparatus of claim 12, comprising means for adaptive setting of said
programmable prediction error filter and/or said random access memory
such that its characteristic automatically adjusts as the colored random
10 noise on said data channel changes.
14. The apparatus of claim 1 or 2 being either completely or partially
implemented in analog circuit technology.
- 15 -15. The apparatus of claim 1 or 2, wherein said feedback means comprise a
feedback finite-impulse response (FIR) filter.
16. The apparatus of claim 1, comprising:
- a memoryless detector for determining a nominal expected value,
 - 20 • means for estimating the noise contribution in a plurality of past
digital samples by subtracting the value of a sample from said
nominal expected value,
 - means for predicting the noise contribution of the current received
sample using the noise contribution in a plurality of said past digital
25 samples,
 - means for adding or subtracting the predicted noise contribution
to/from the current received sample, and
 - means for feeding the output of the means for adding or subtracting
to a conventional partial response maximum likelihood (PRML) or
30 extended partial-response maximum likelihood (EPRML) detector.

- 1 17. The apparatus of any of the claims 1-16, wherein said channel is a data
transmission channel and said apparatus is employed for estimation of
data received via said data transmission channel.
- 5 18. Direct access storage device, in particular a disk drive, comprising direct
access storage means and an apparatus for noise predictive maximum
likelihood (NPML) sequence detection according to any of the claims 1 -
16, said channel being a storage channel for feeding signals retrieved
from said direct access storage means to said apparatus.
- 10 19. The apparatus of any of the claims 1-16, being integrated into
(piggy-backed) on a partial-response maximum likelihood (PRML) or
extended partial-response maximum likelihood (EPRML) system.
- 15 20. The apparatus of claim 19, wherein a digital equalizer, being part of said
partial-response maximum likelihood (PRML) or extended
partial-response maximum likelihood (EPRML) system, and said prediction
error filter are replaced by a single finite-impulse response filter having
the property to whiten said colored random noise components of said
20 sample y_n .
- 25 21. The apparatus of any of the claims 1-16, being connected to a partial
response maximum likelihood (PRML) or an extended partial-response
maximum likelihood (EPRML) detector such that one can switch from a
first state where the apparatus and either one of said detectors operate
concurrently to a second state where either said partial response
maximum likelihood (PRML) or extended partial-response maximum
likelihood (EPRML) detector, or said apparatus processes said sample y_n
received via said channel.
- 30 22. Method for noise predictive maximum likelihood (NPML) sequence
detection by means of a sequence detector having a state complexity
being equal to 2^K , with $0 \leq K \leq L$, said method comprising the steps:

- 1 a) whitening colored random noise components of a sample y_n received
via a channel, said sample y_n comprising a generalized partial
response signal component corrupted by said colored random noise
components, leading to a signal z_n then having L
5 intersymbol-interference components.
- b) eliminating K of said L intersymbol-interference components by
carrying out a branch metric computation based on a 2^K -State Viterbi
algorithm to determine the most likely sequence corresponding to
said sample y_n , and
- 10 c) if there are any intersymbol-interference components left, i.e., if
 $L - K > 0$,
- precomputing intersymbol-interference cancellation terms,
 - storing said intersymbol-interference cancellation terms in
storage means,
 - 15 • retrieving said intersymbol-interference cancellation terms from
said storage means by applying path history decisions from said
sequence detector as addresses to said memory means,
 - cancelling said L-K intersymbol-interference components in said
signal z_n using said intersymbol interference cancellation terms.

20

23. The method of claim 22, comprising the steps:

- estimating the noise contribution in a plurality of past digital samples
by subtracting the value of a sample from a nominal expected value,
said nominal expected value being determined by simple
25 memoryless detection,
- using the noise contribution in a plurality of said past digital samples
to predict the noise contribution of the current received sample,
- adding or subtracting the predicted noise contribution to/from the
current received sample, and
- 30 • feeding the output of the last step to a conventional partial response
maximum likelihood (PRML) or extended partial-response maximum
likelihood (EPRML) detector.

- 1 24. The method of claim 22, wherein said sample y_n received via said channel
is a partial-response signal and in particular a partial-response class-4
(PR4) shaped signal.

5

10

15

20

25

30

1/27

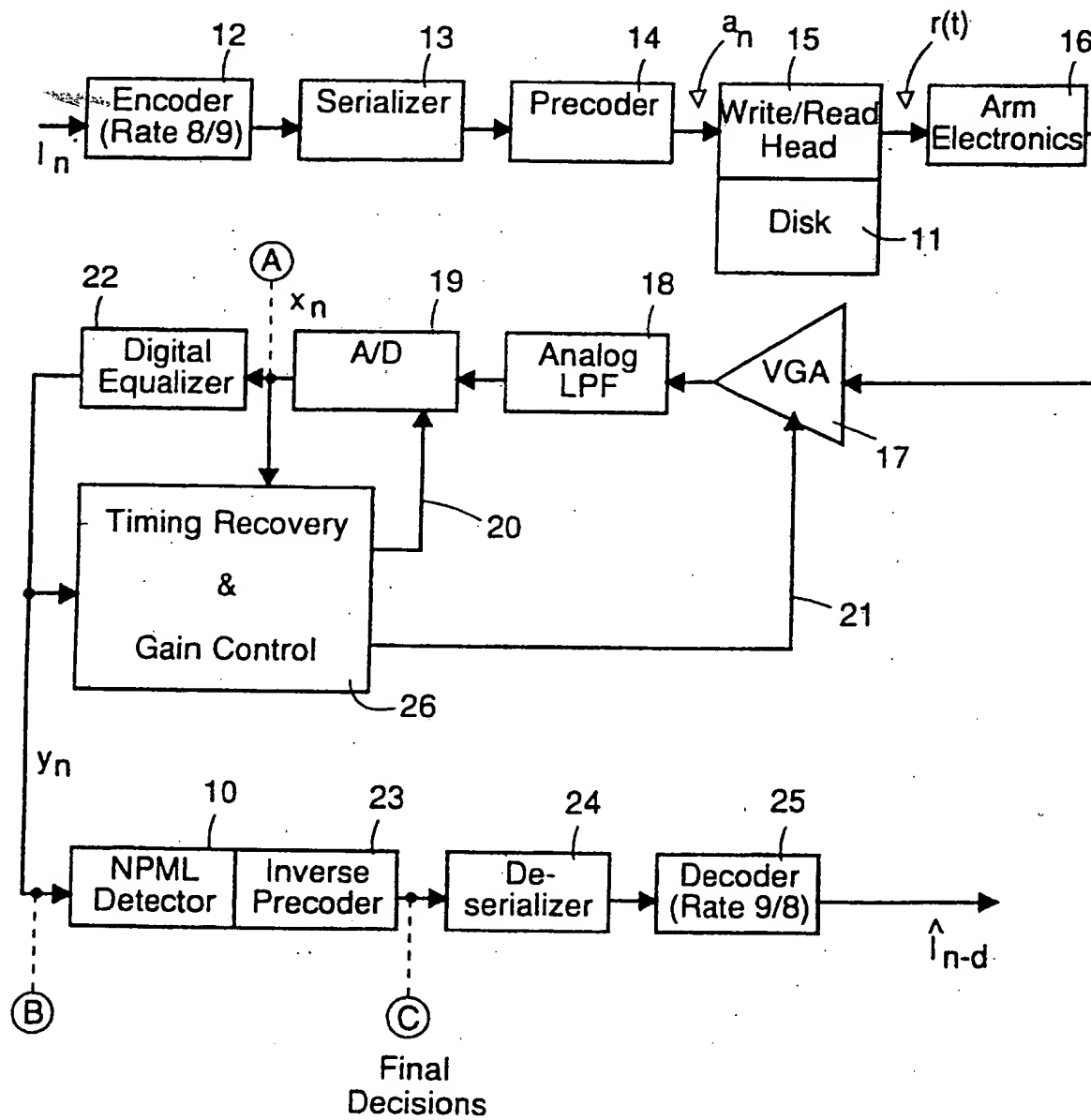


FIG. 1

2/27

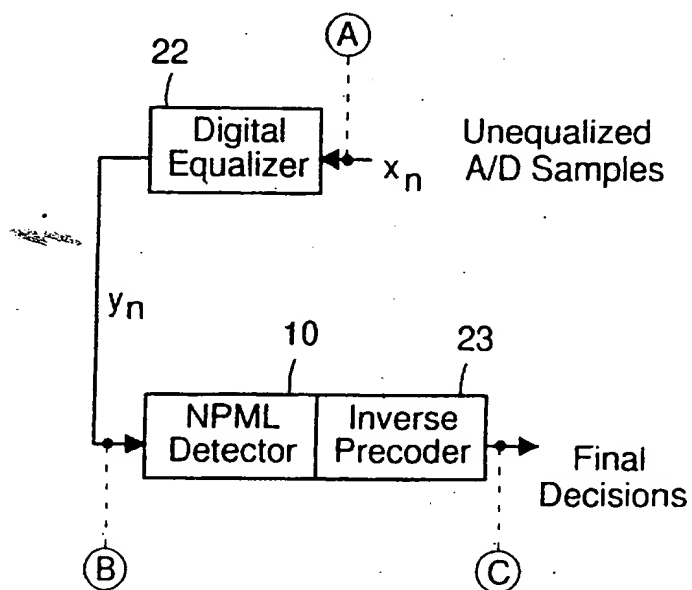


FIG. 2A

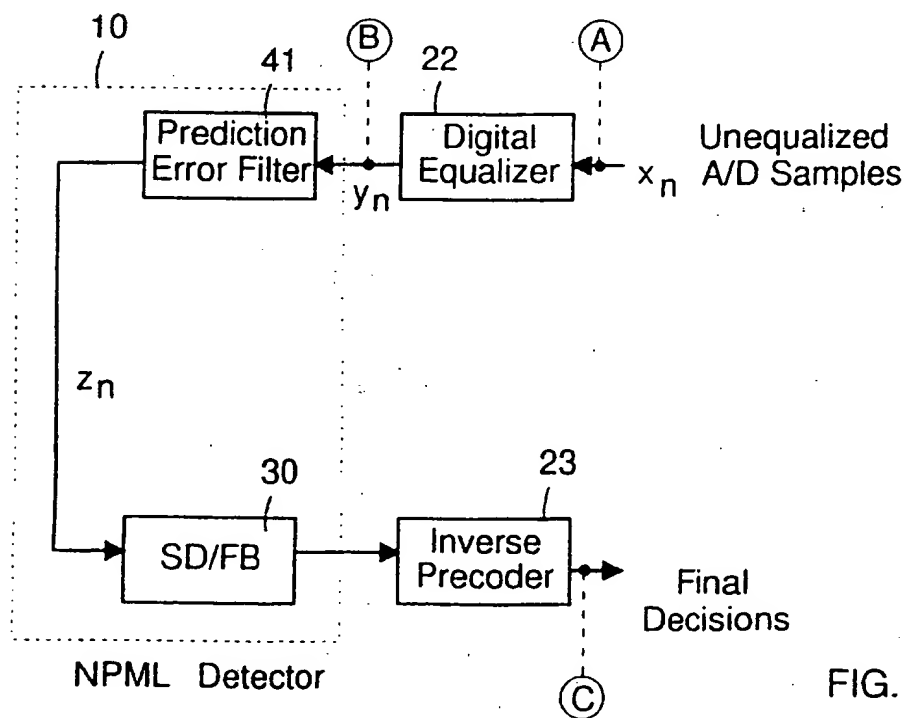
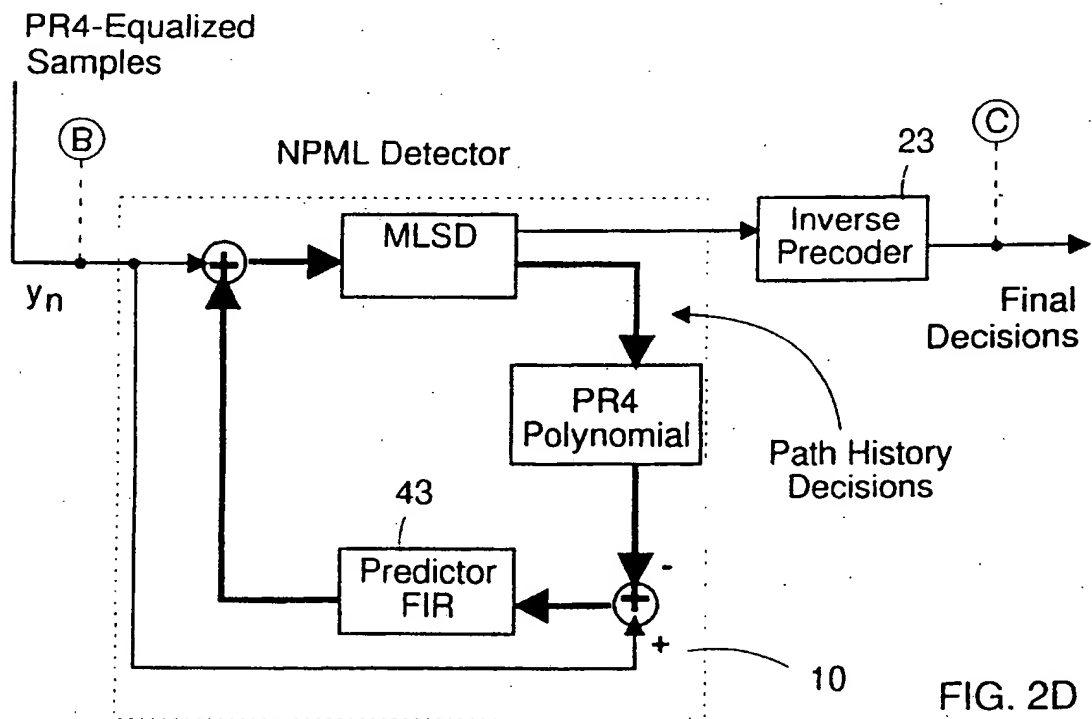
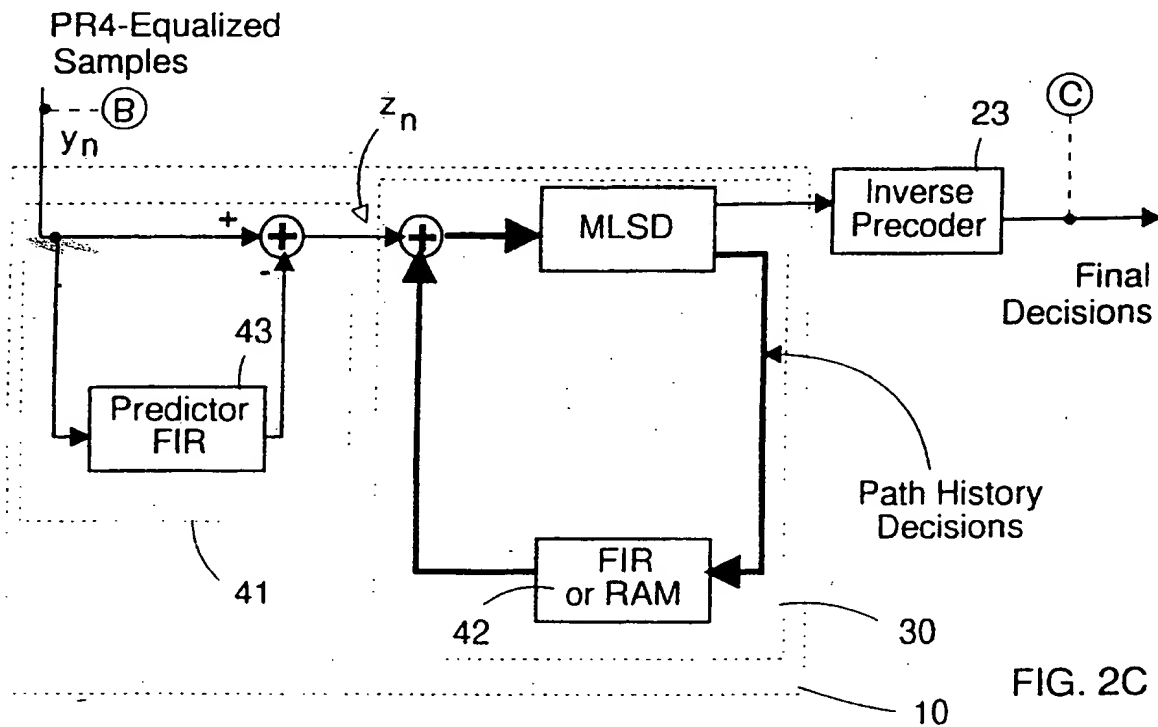


FIG. 2B

3/27



4/27

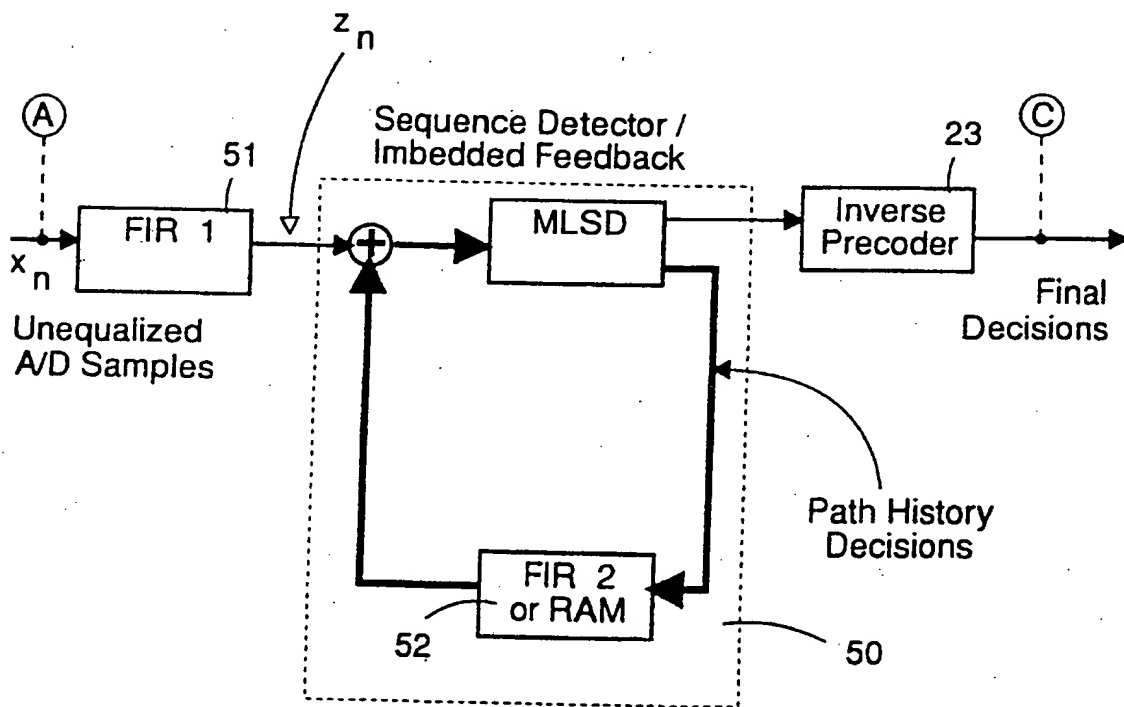


FIG. 2E

5/27

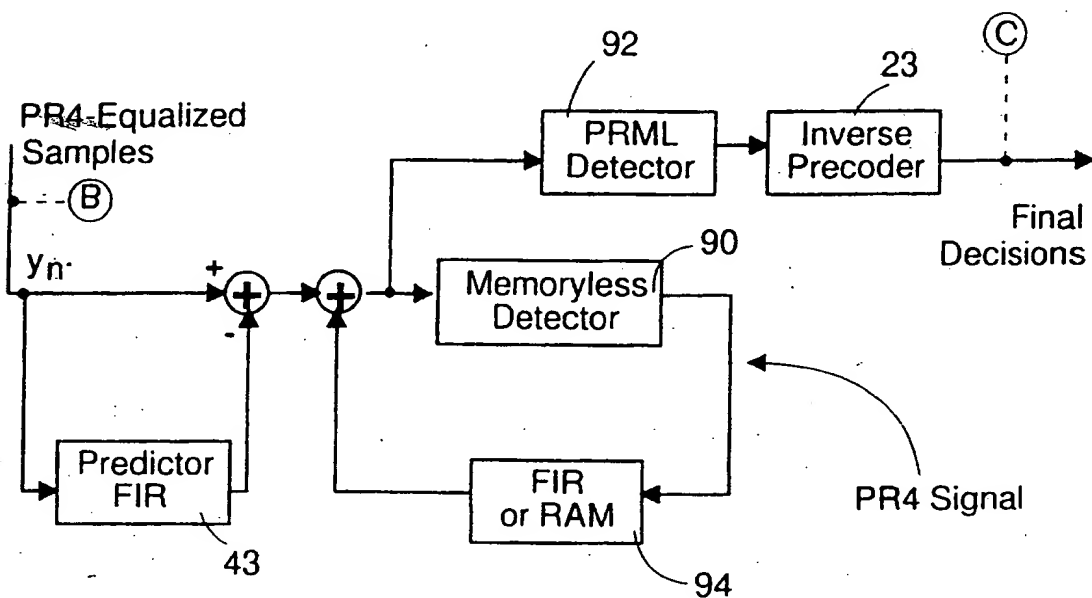


FIG. 3A

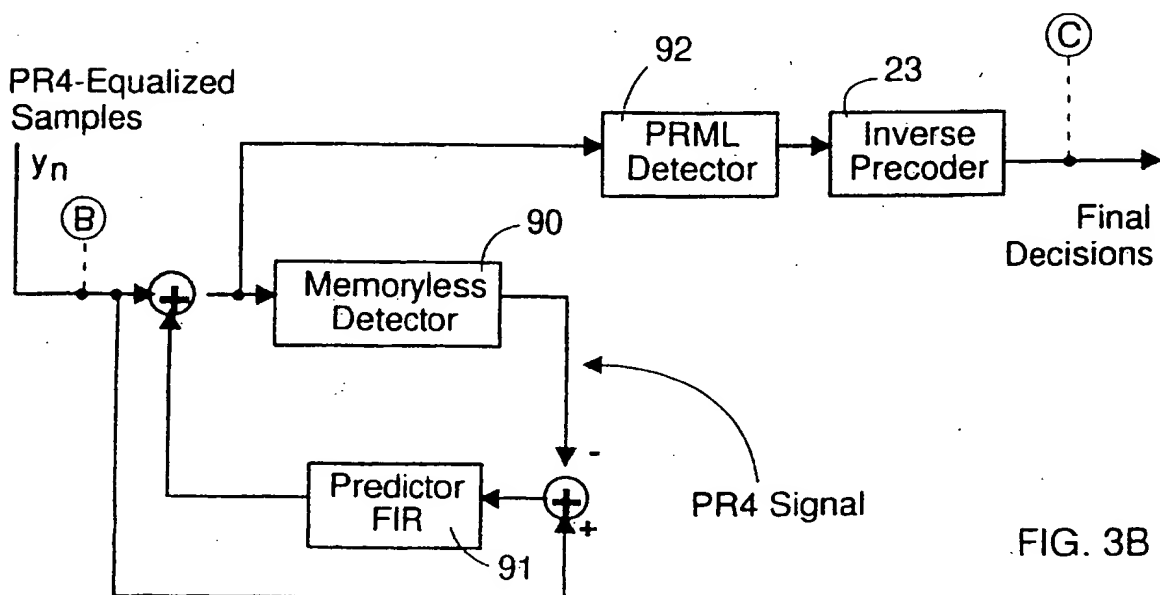


FIG. 3B

6/27

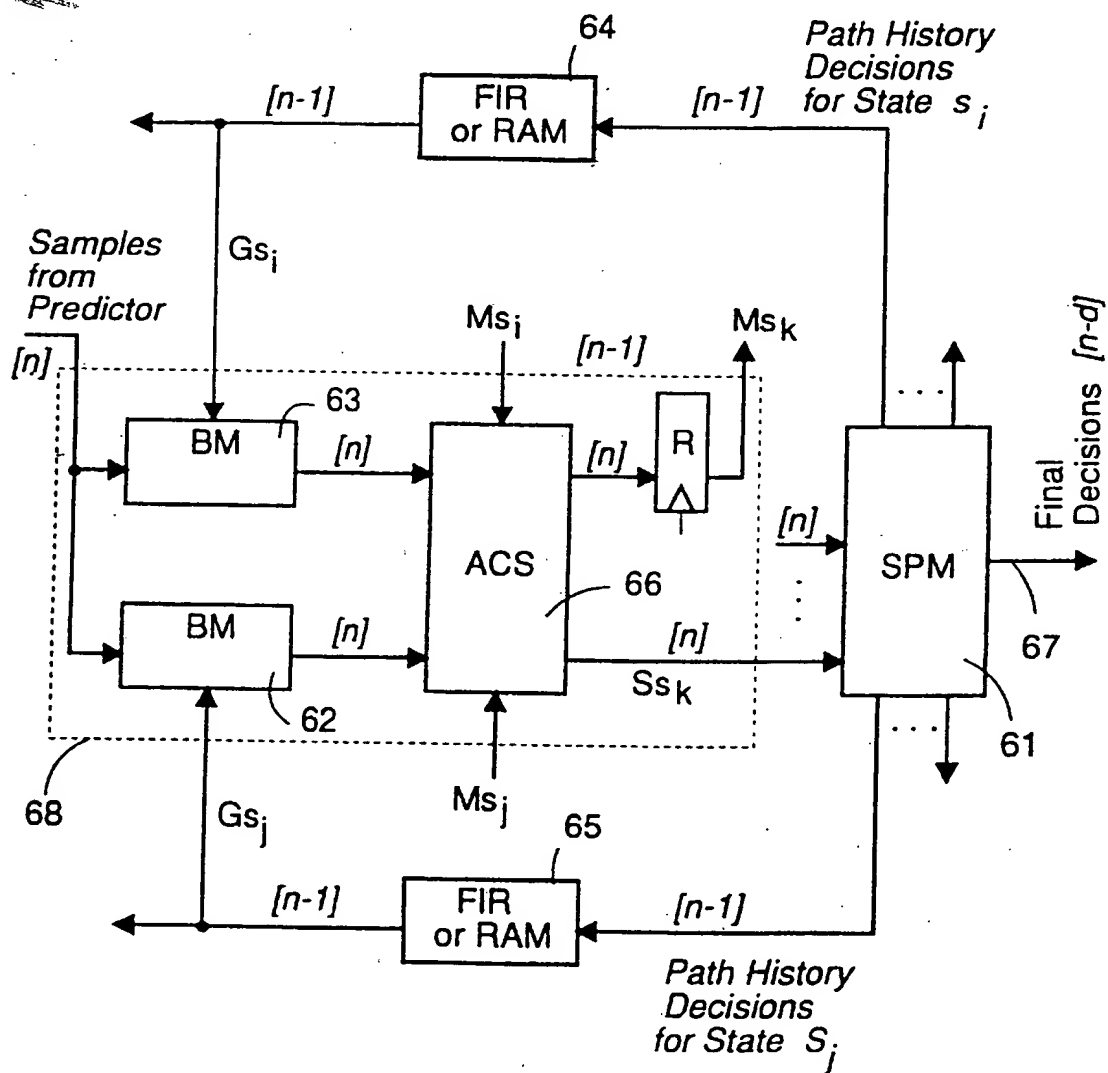


FIG. 4

7/27

NPML : 2-State Trellis

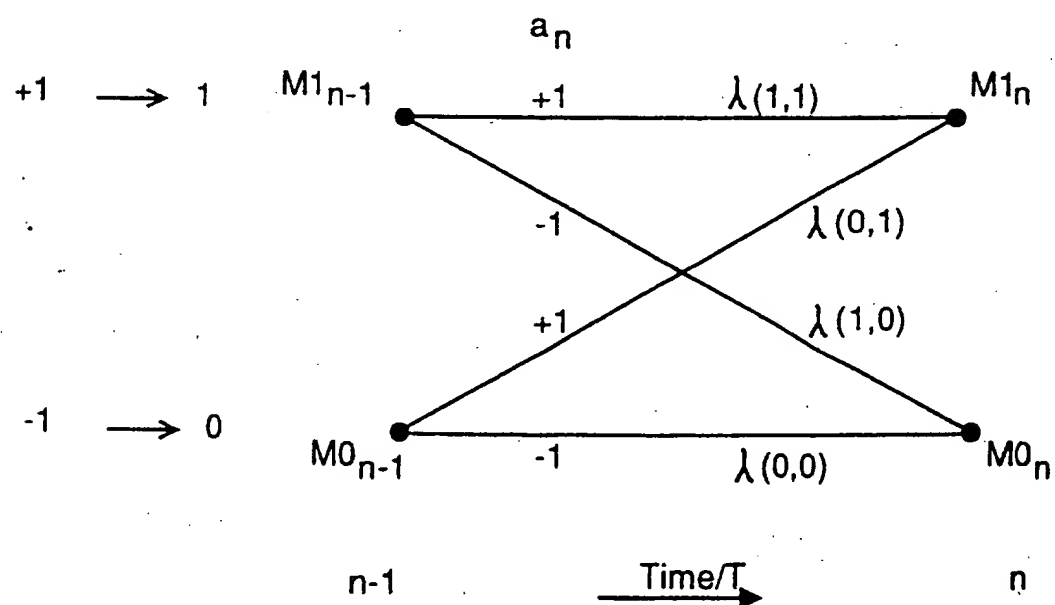
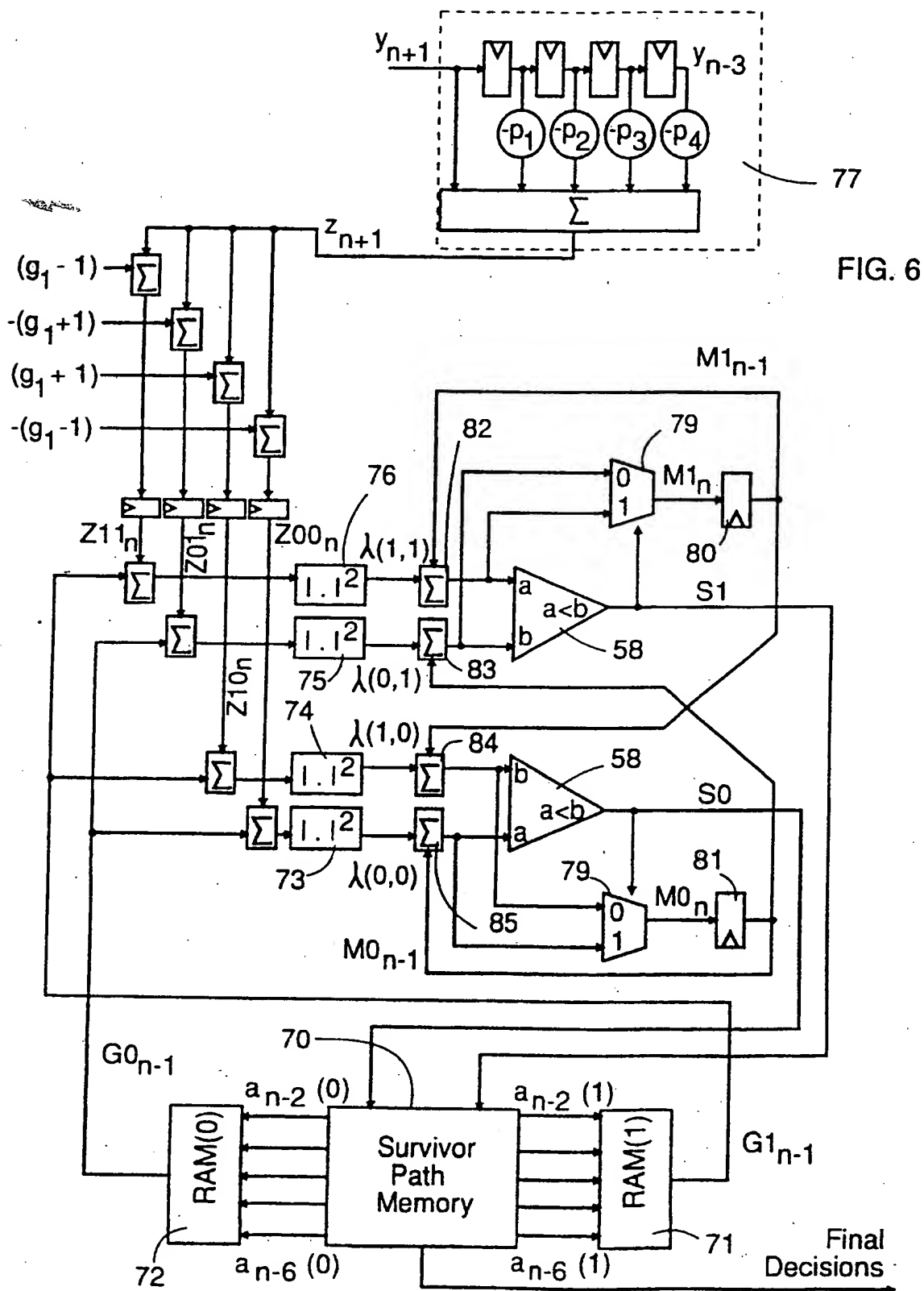
 $a_{n-1} \longrightarrow \text{state}$ 

FIG. 5

8/27



9/27

NPML : 2-State Trellis (Difference Metric)

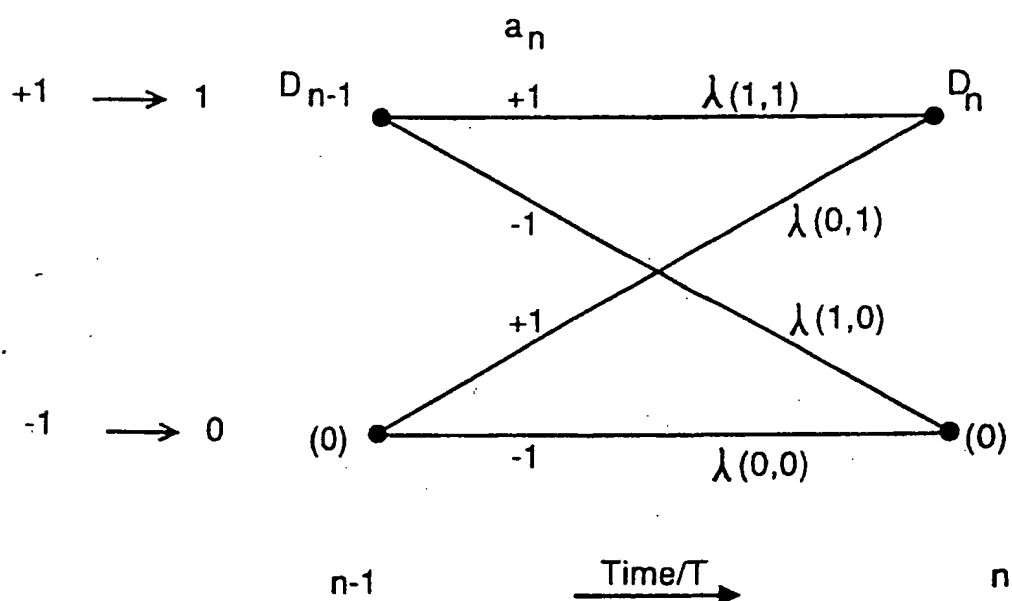
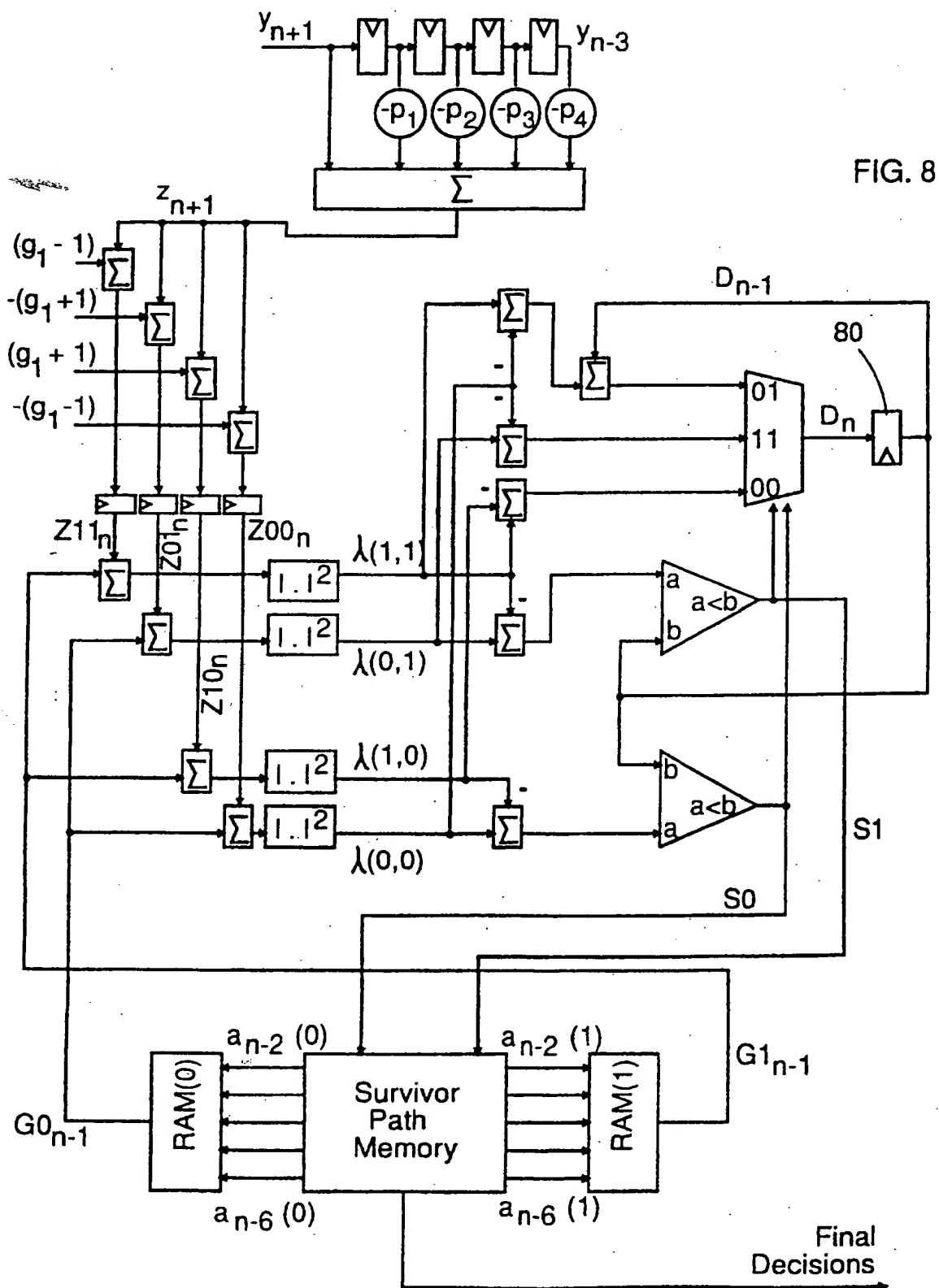
 $a_{n-1} \longrightarrow \text{state}$ 

FIG. 7

10/27



11/27

NPML : 4-State Trellis

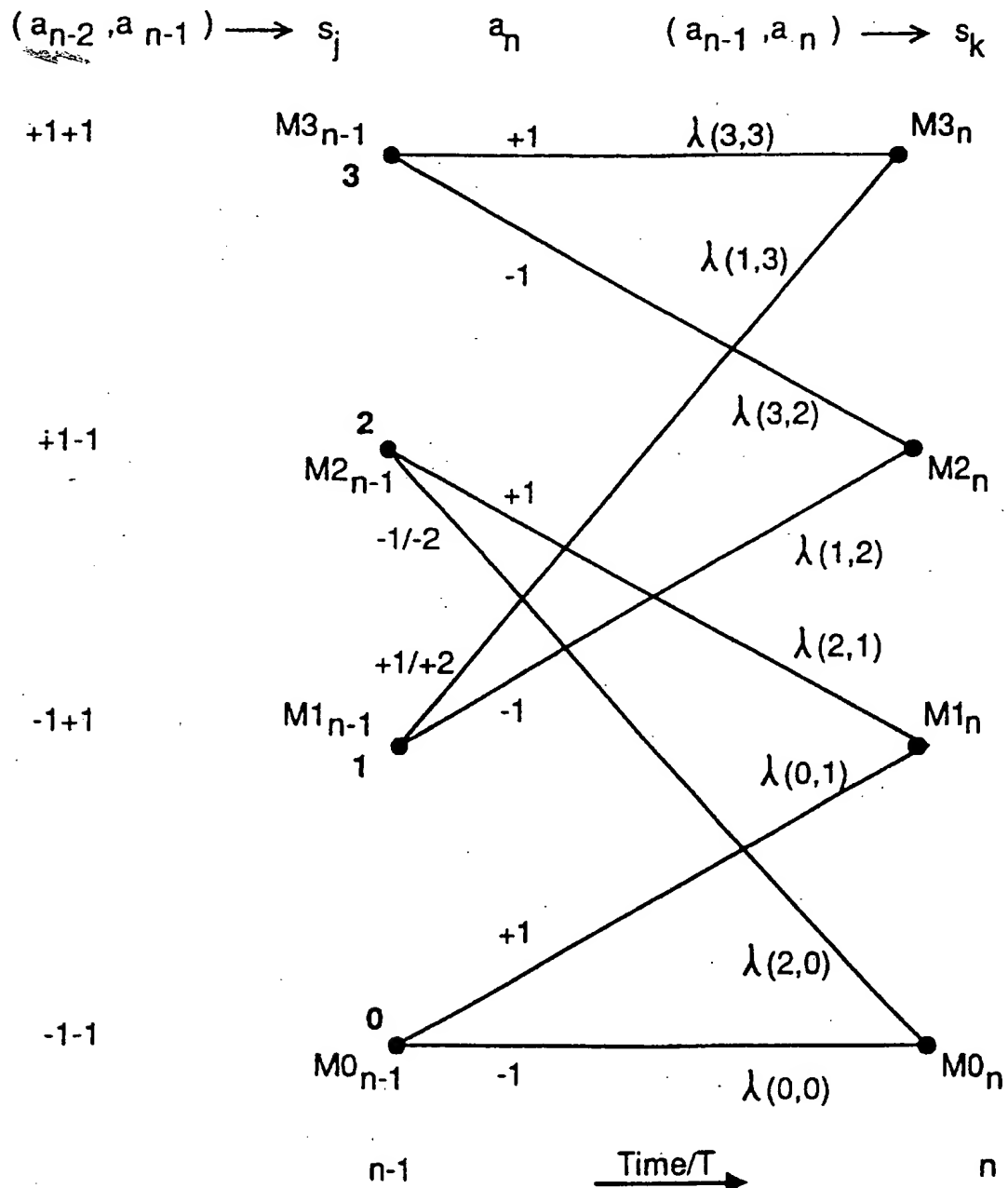
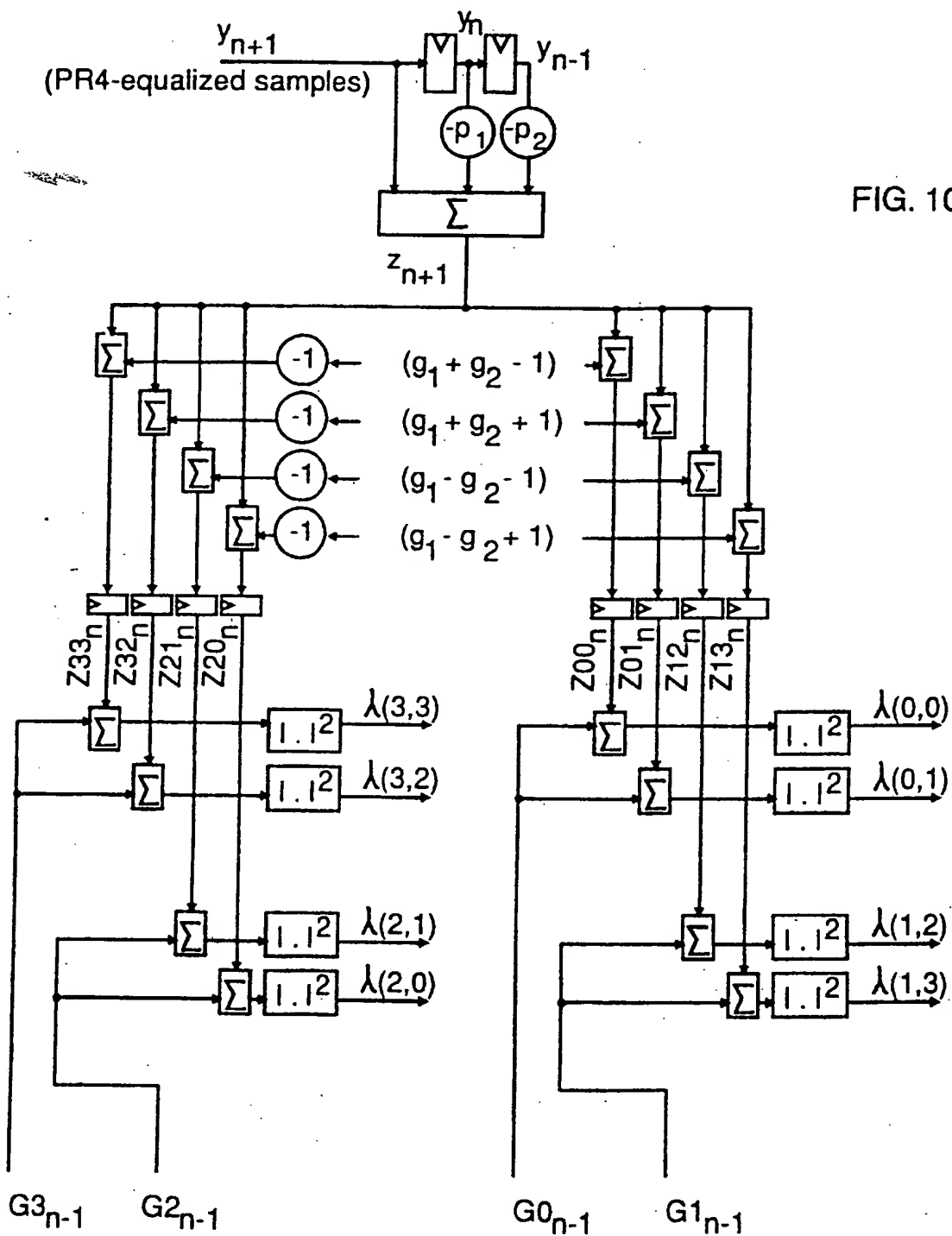


FIG. 9

12/27



13/27

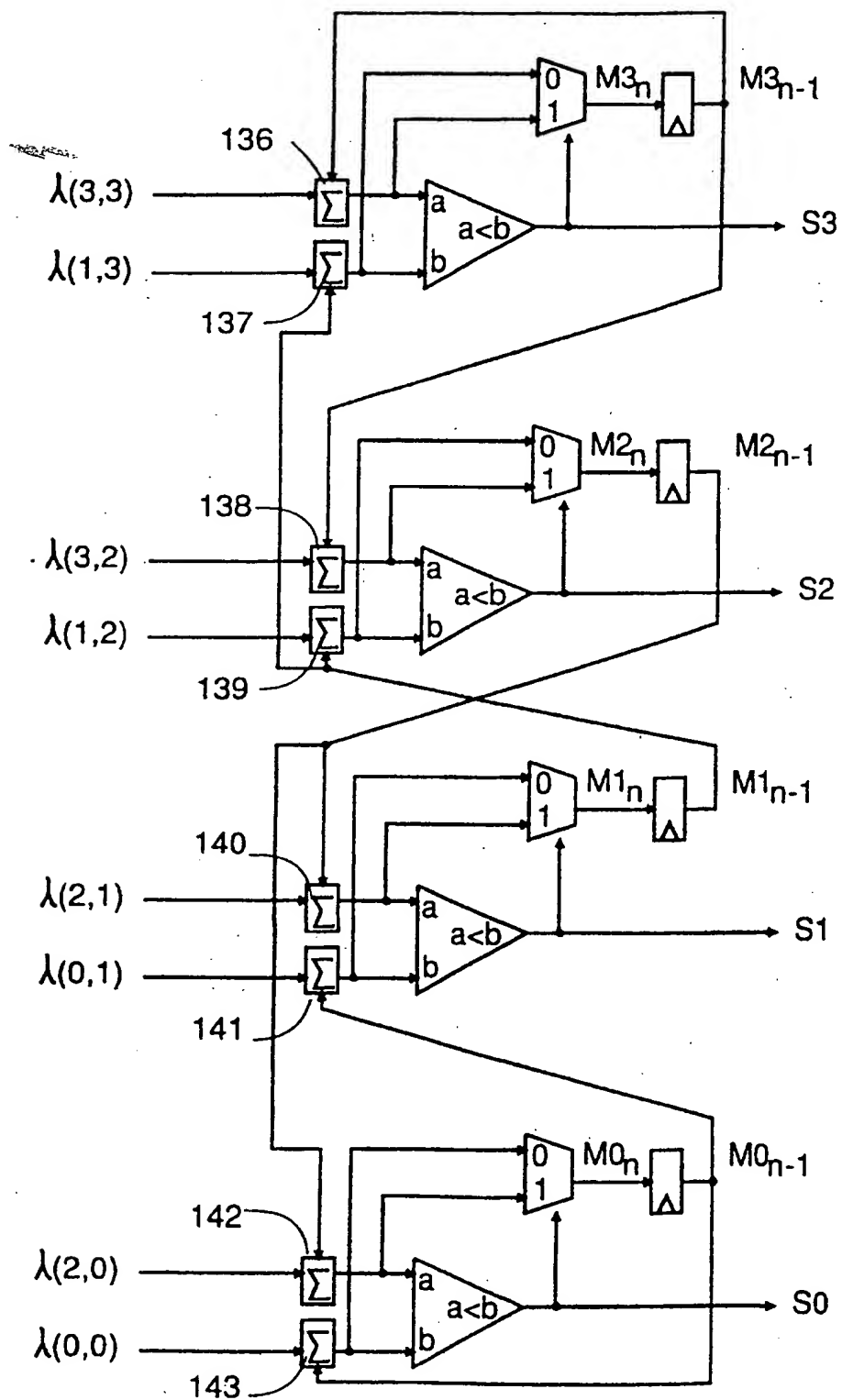
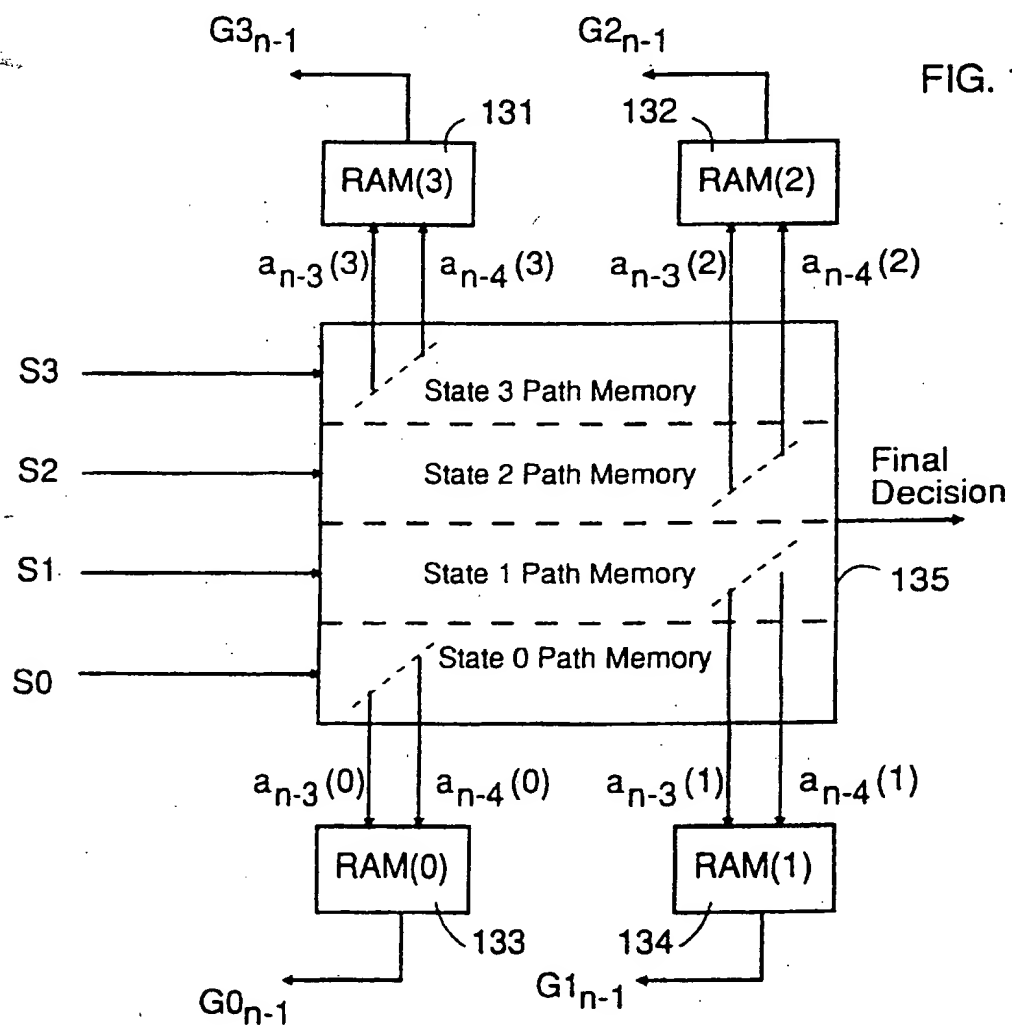
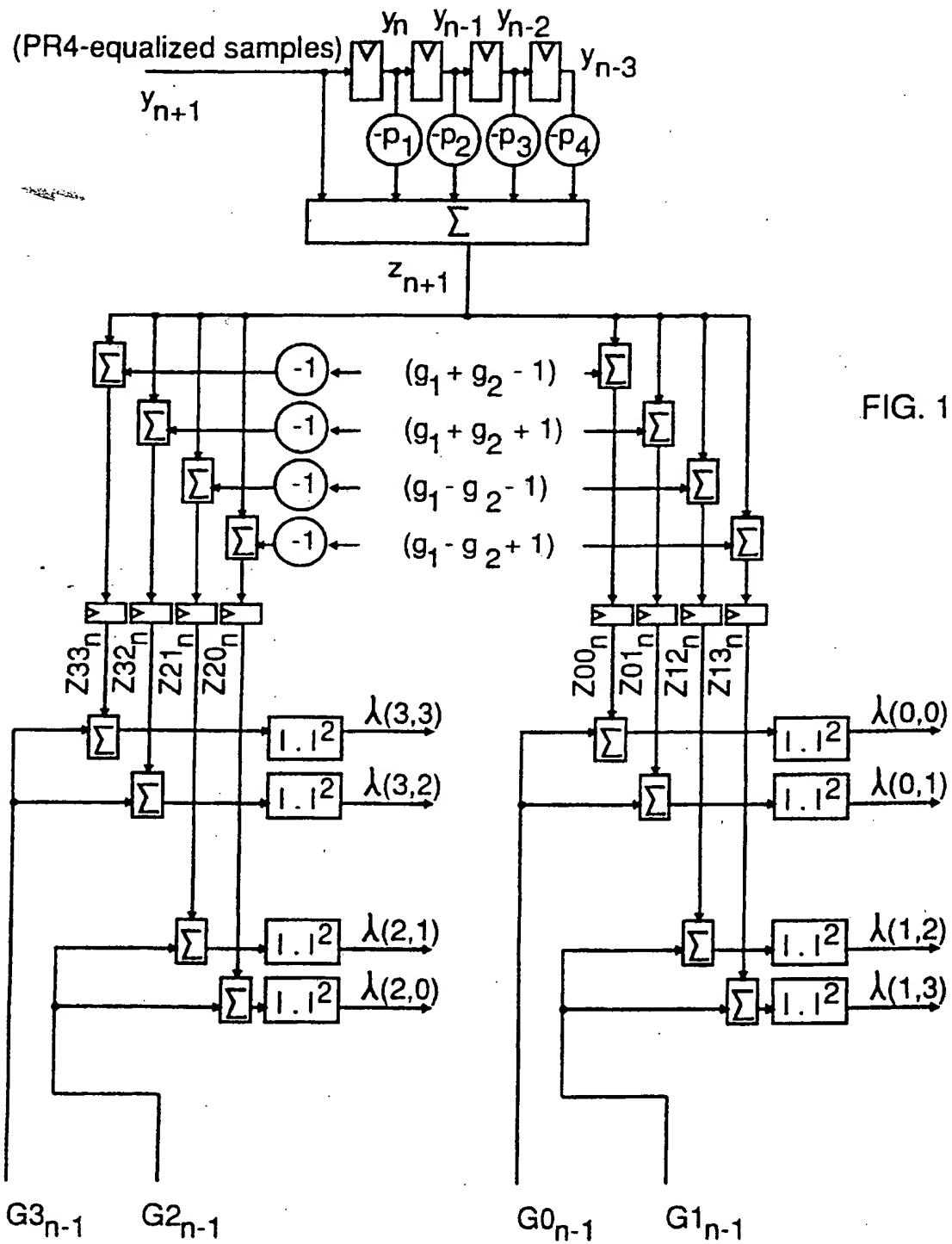


FIG. 10B

14/27



15/27



16/27

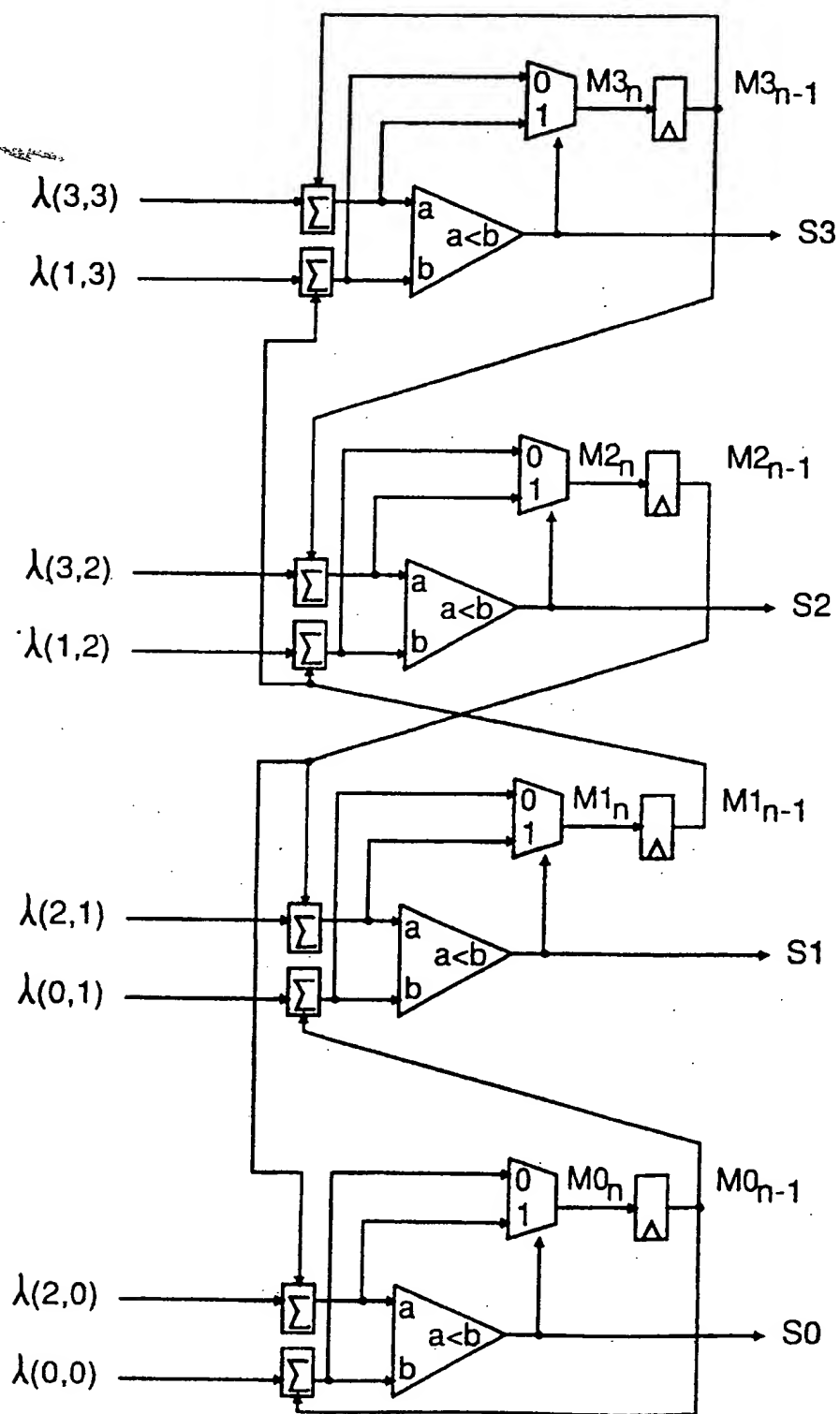
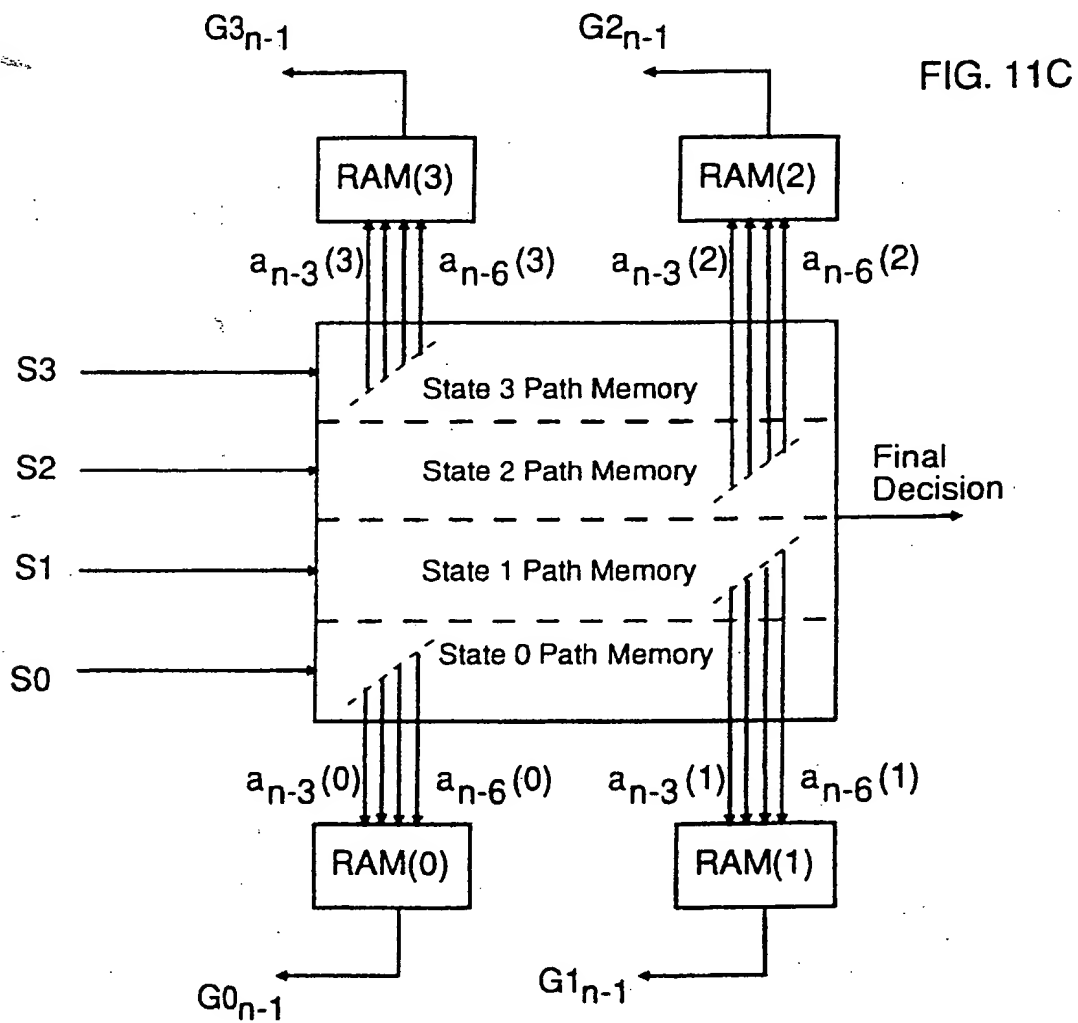


FIG. 11B

17/27



18/27

NPML : 8-State Trellis (N=1, K=3)

$$s_j \leftarrow (a_{n-3}, a_{n-2}, a_{n-1}) \quad (a_{n-2}, a_{n-1}, a_n) \rightarrow s_k$$

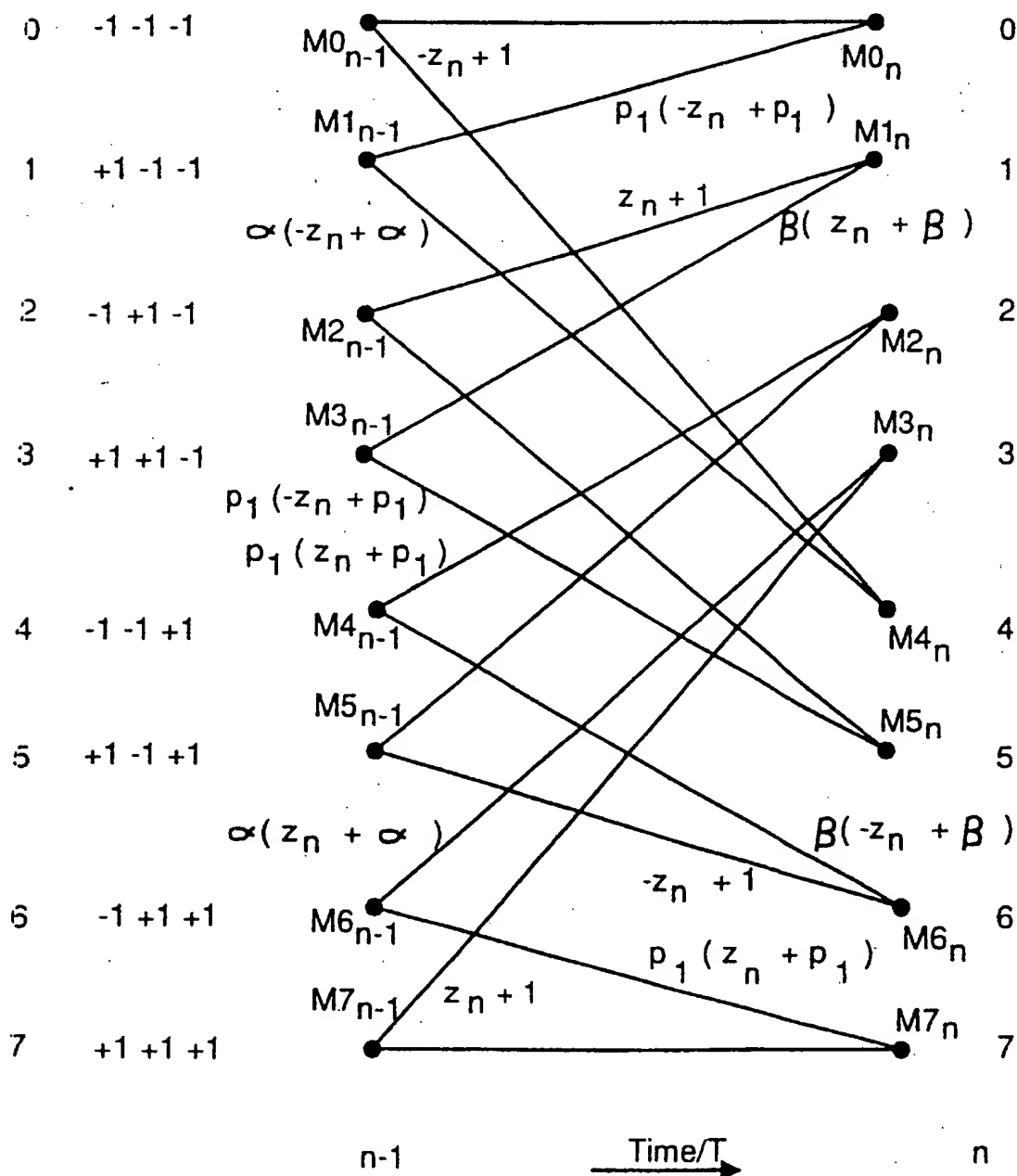


FIG. 12

19/27

NPML : Transformed 8-State Trellis (N=1, K=3)

$$s_j \leftarrow (a_{k-3}, a_{k-2}, a_{k-1})$$

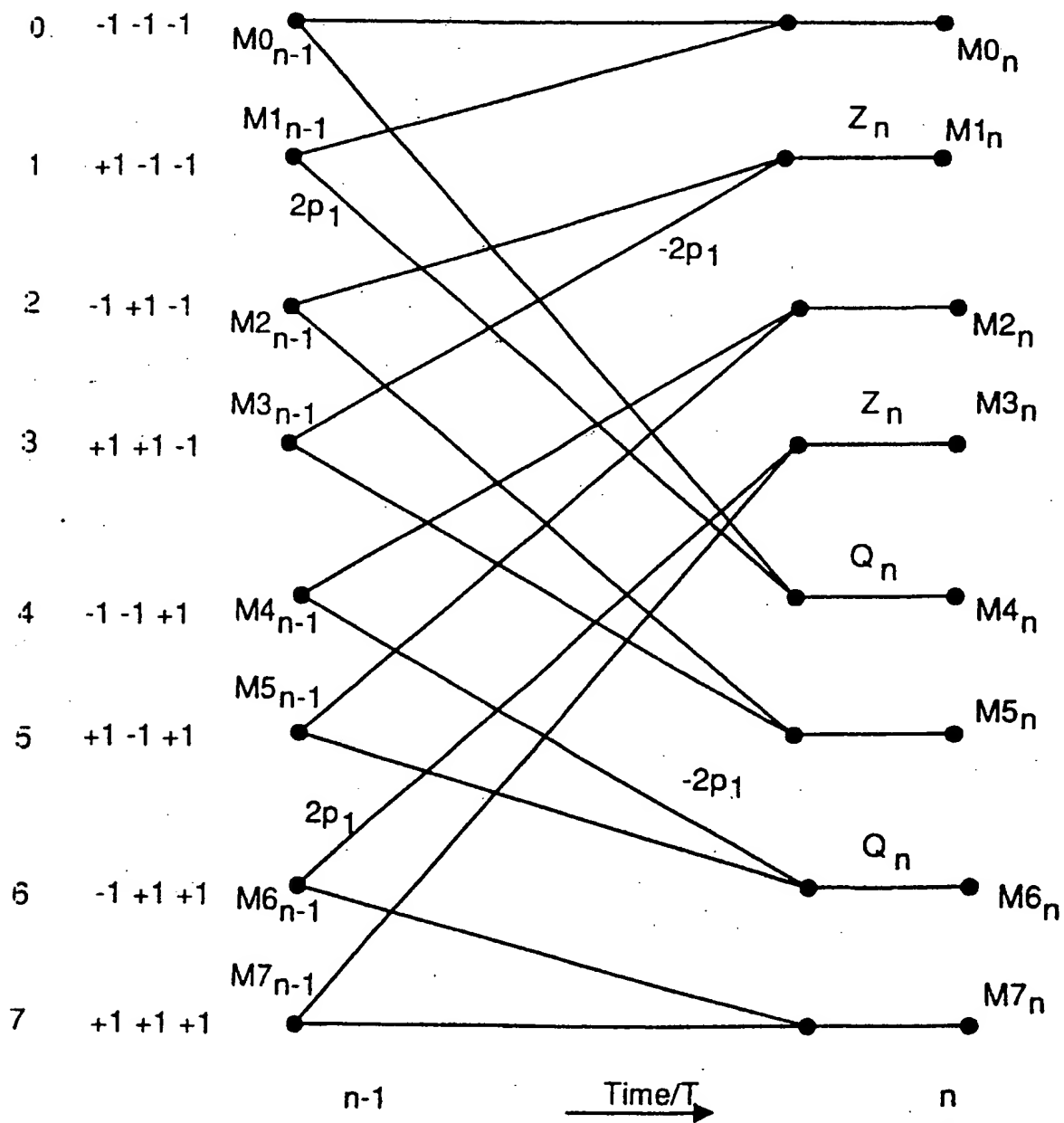


FIG. 13.

20/27

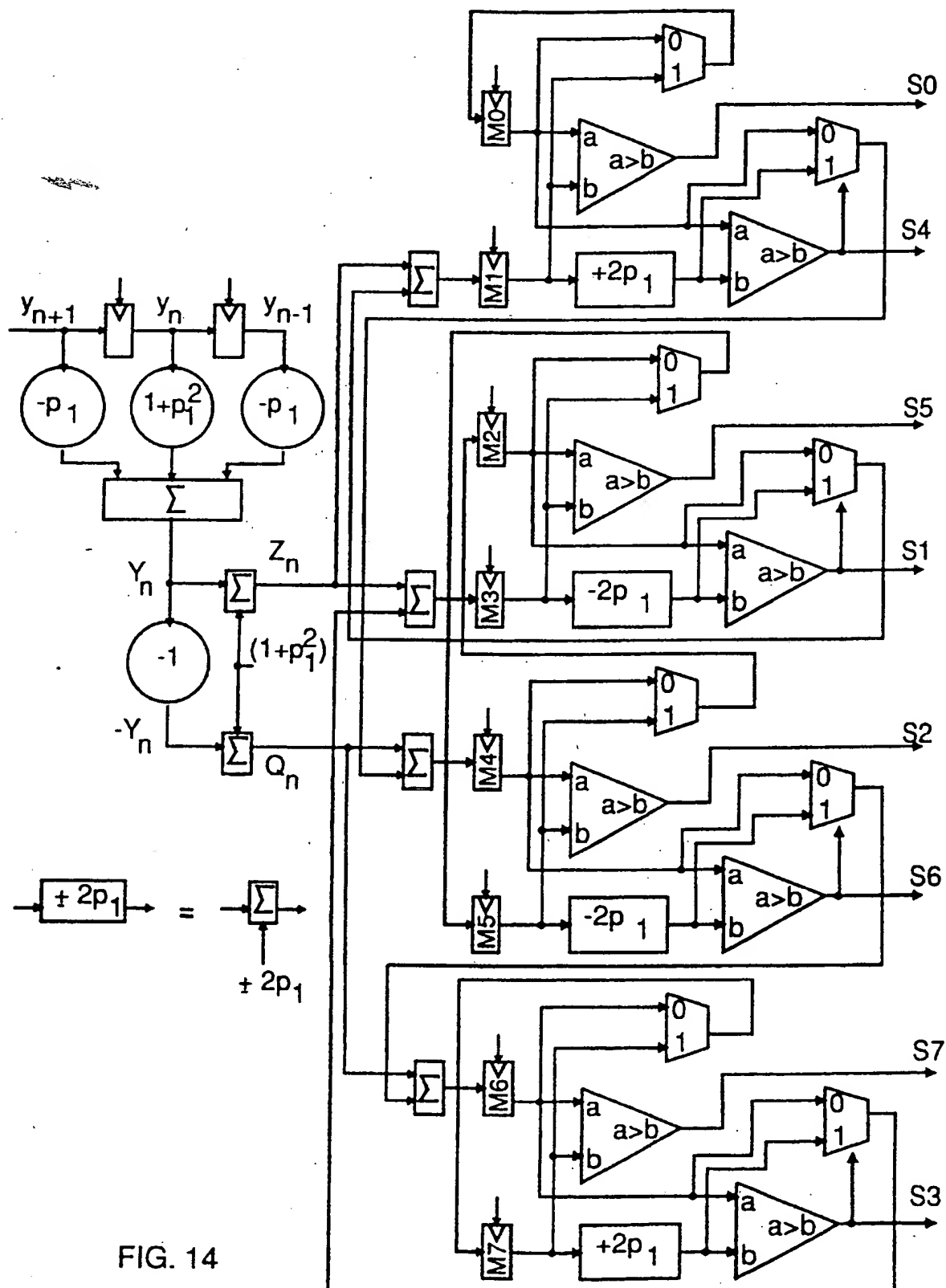
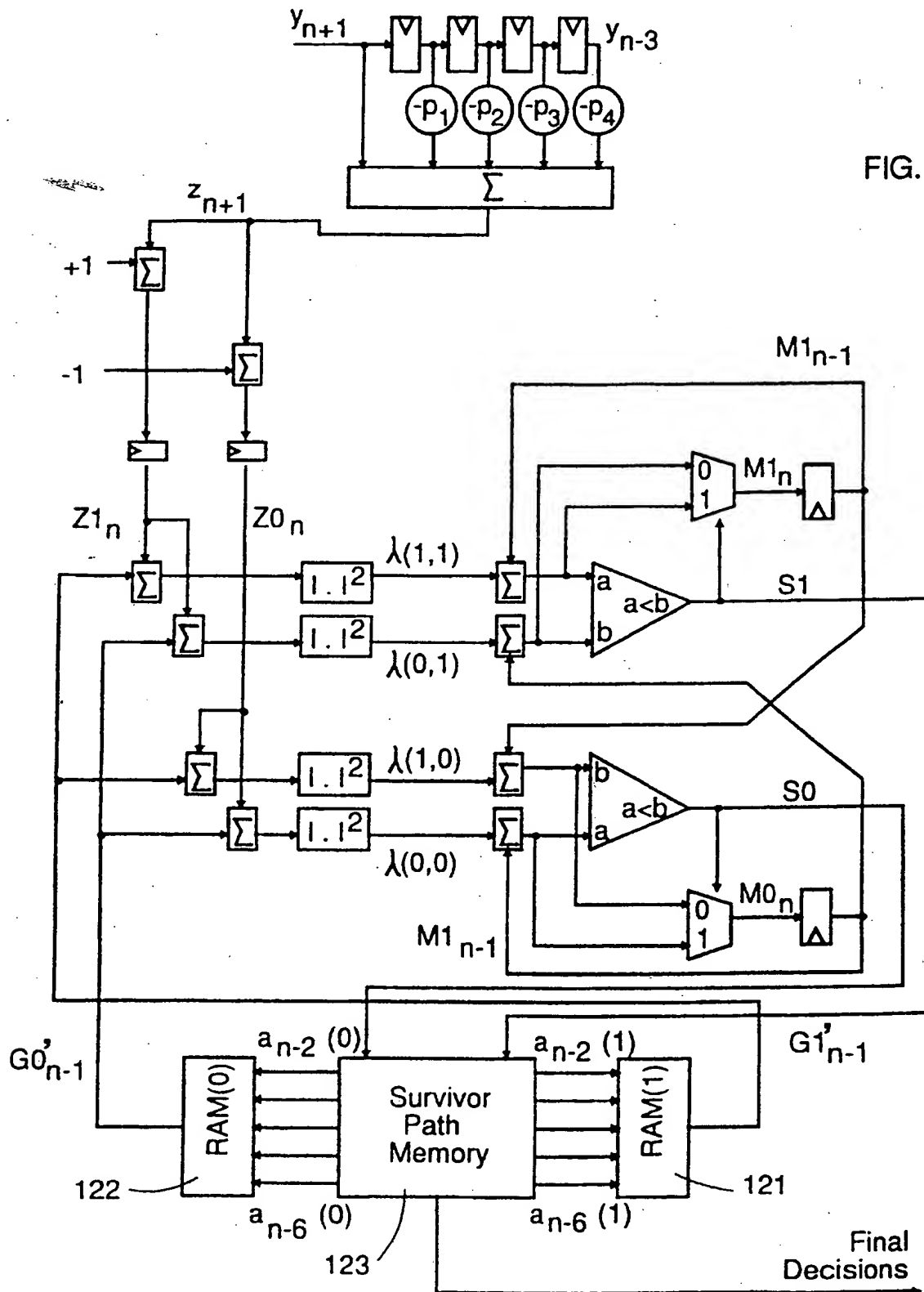


FIG. 14

21/27

FIG. 15



22/27

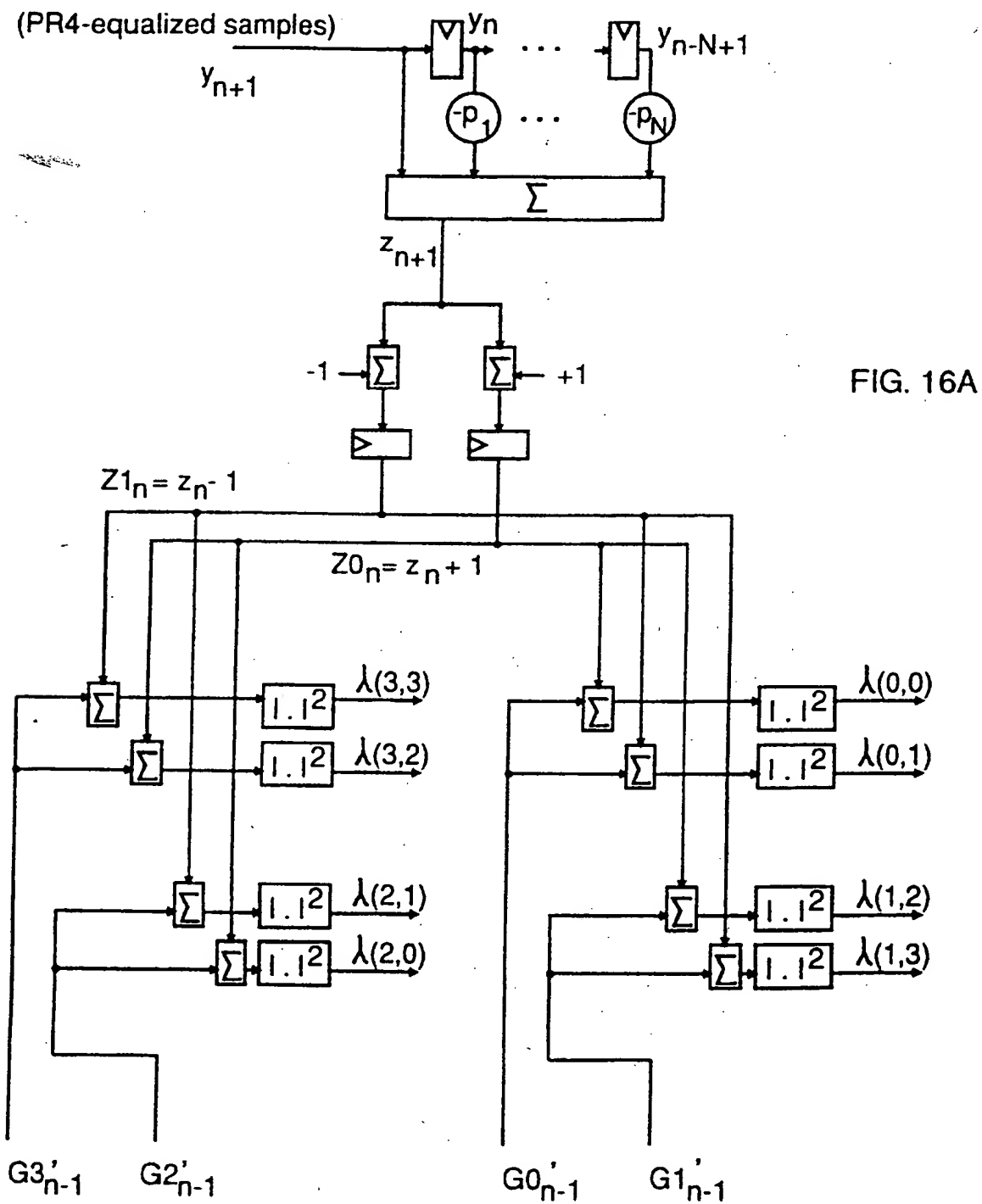


FIG. 16A

23/27

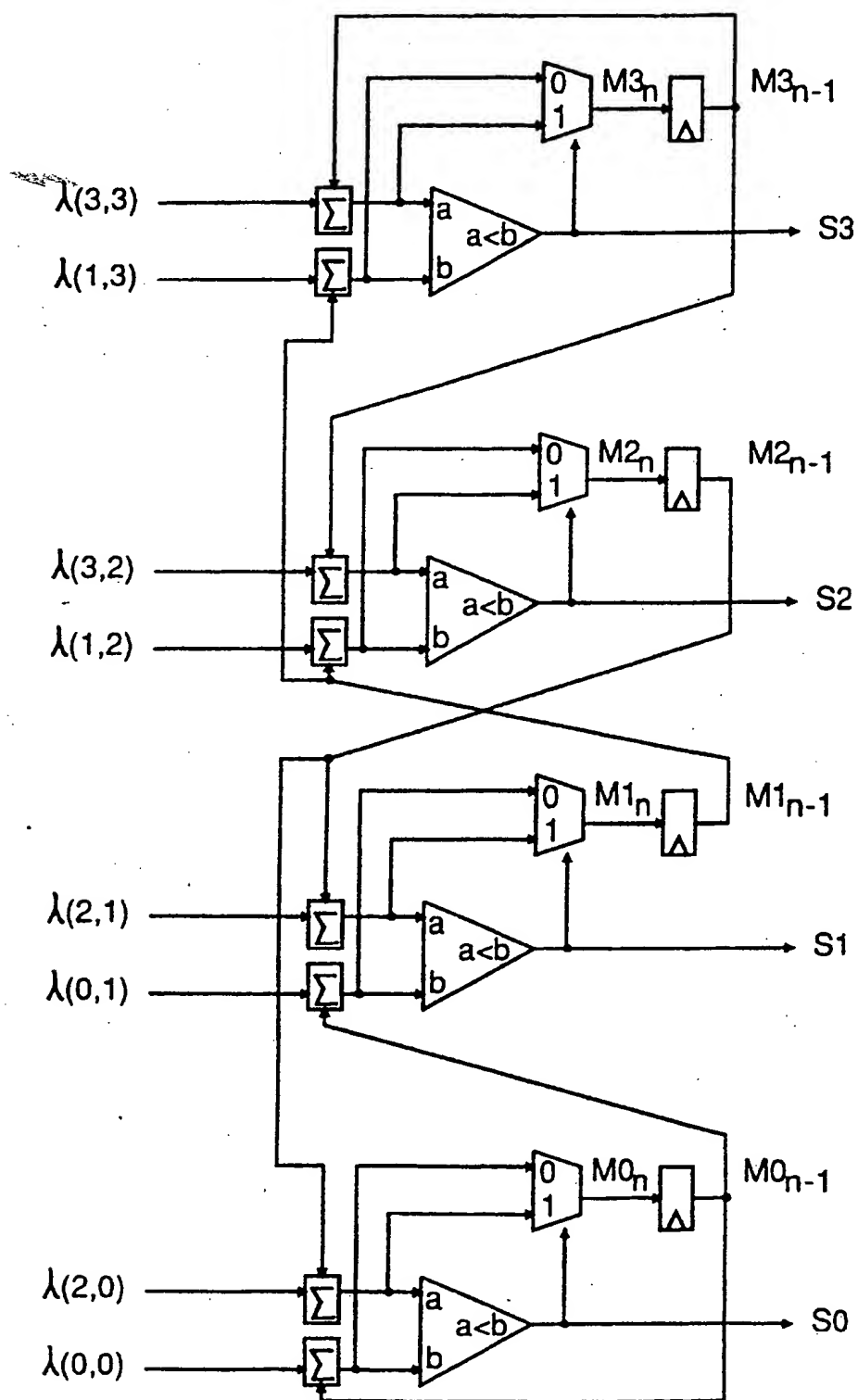
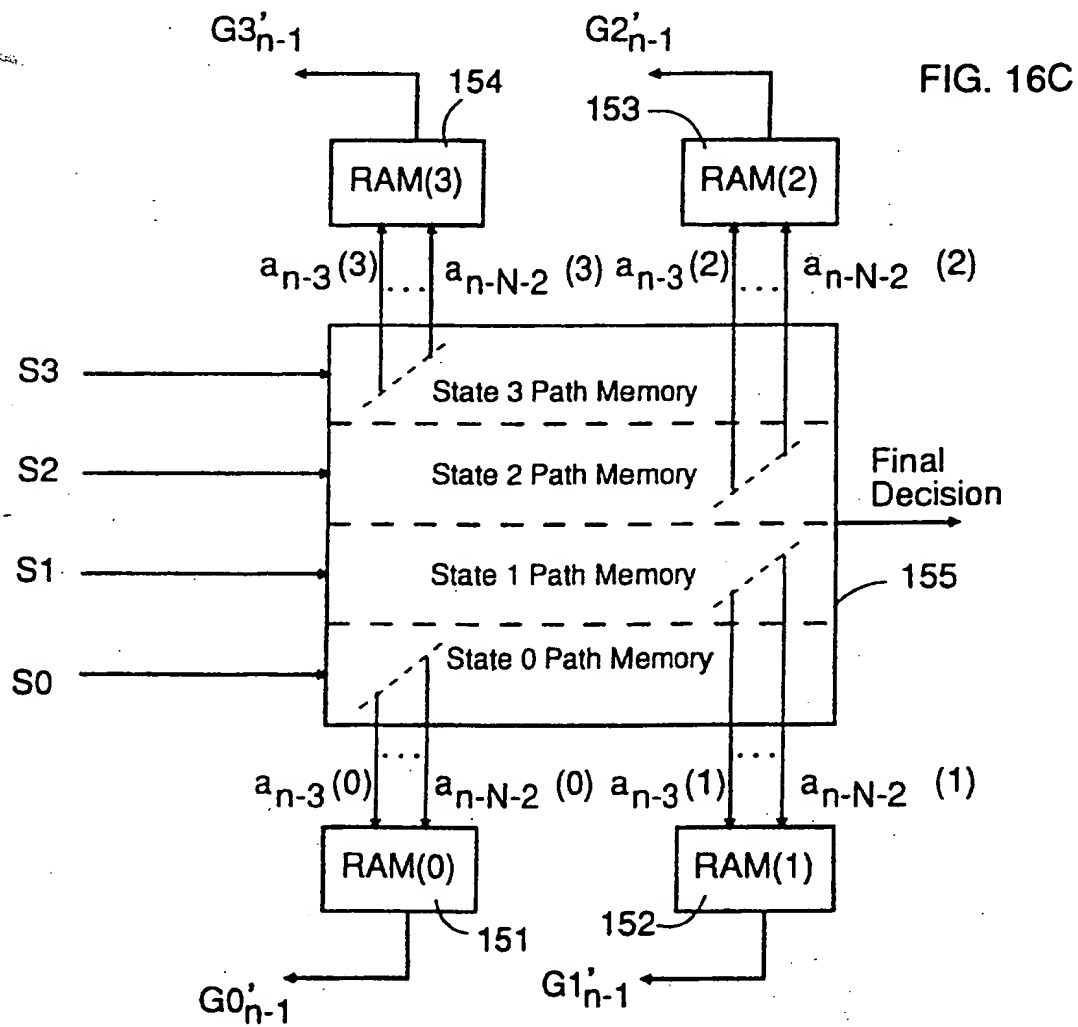
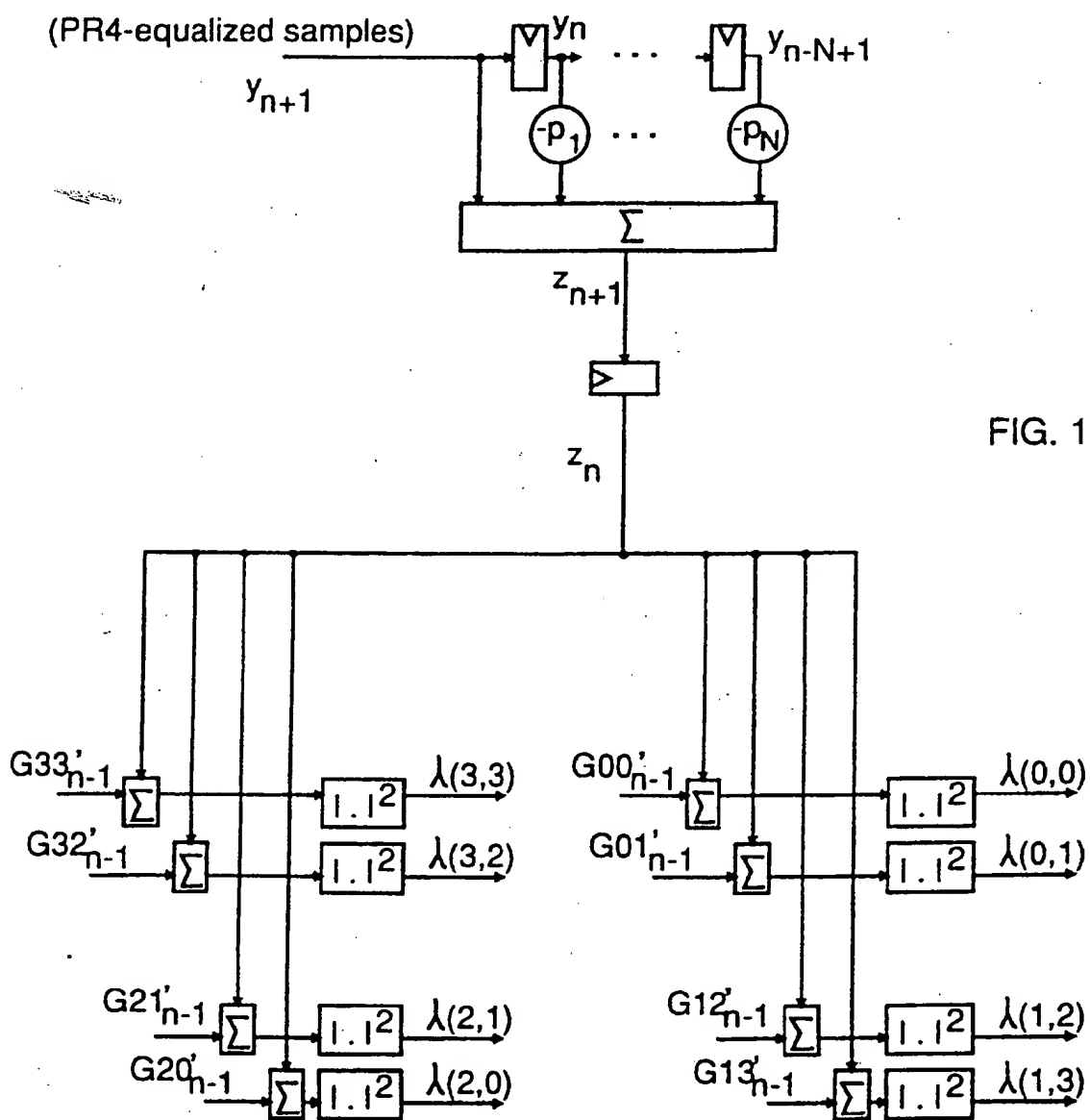


FIG. 16B



25/27



26/27

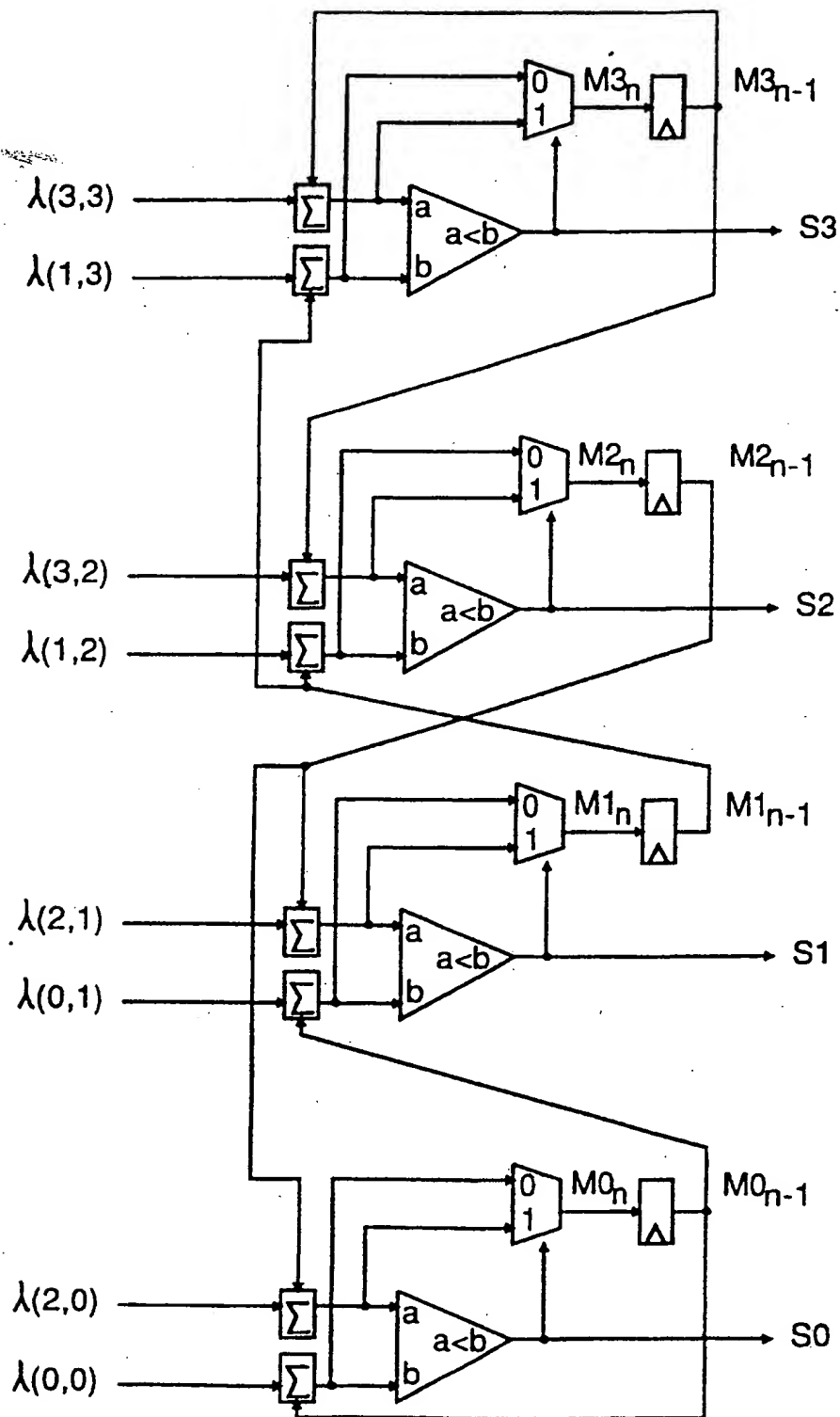
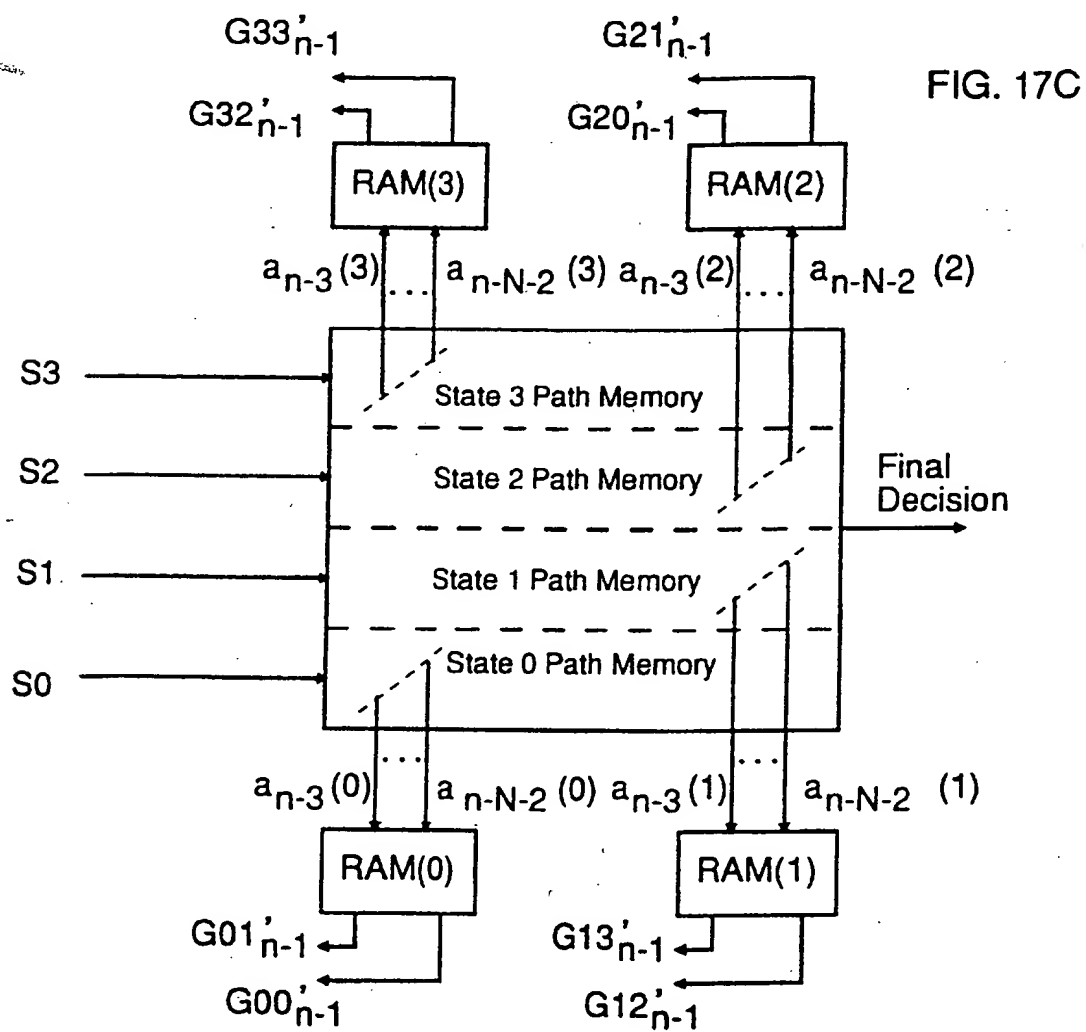


FIG. 17B

27/27



INTERNATIONAL SEARCH REPORT

International Application No
PCT/IB 95/00769

A. CLASSIFICATION OF SUBJECT MATTER IPC 6 H04L25/03 H04L25/497		
According to International Patent Classification (IPC) or to both national classification and IPC		
B. FIELDS SEARCHED		
Minimum documentation searched (classification system followed by classification symbols) IPC 6 H04L		
Documentation searched other than minimum documentation to the extent that such documents are included in the fields searched		
Electronic data base consulted during the international search (name of data base and, where practical, search terms used)		
C. DOCUMENTS CONSIDERED TO BE RELEVANT		
Category *	Citation of document, with indication, where appropriate, of the relevant passages	Relevant to claim No.
A	WO,A,94 29989 (IBM ;CHEVILLAT PIERRE (CH); ELEFThERIOU EVANGELOS (CH); MAIWALD DI) 22 December 1994 cited in the application see the whole document	1-24
A	PROCEEDINGS OF THE INTERNATIONAL CONFERENCE ON COMMUNICATIONS, ICC'92, CHICAGO, JUNE 14-18, 1992, vol. 2 OF 4, 14 June 1992, INSTITUTE OF ELECTRICAL AND ELECTRONICS ENGINEERS, pages 942-947, XP000326811 CHEVILLAT P. R. ET AL: "NOISE-PREDICTIVE PARTIAL-RESPONSE EQUALIZERS AND APPLICATIONS" cited in the application see the whole document --- -/--	1-24
<input checked="" type="checkbox"/> Further documents are listed in the continuation of box C. <input checked="" type="checkbox"/> Patent family members are listed in annex.		
<p>* Special categories of cited documents:</p> <p>"A" document defining the general state of the art which is not considered to be of particular relevance</p> <p>"E" earlier document but published on or after the international filing date</p> <p>"L" document which may throw doubts on priority claim(s) or which is cited to establish the publication date of another citation or other special reason (as specified)</p> <p>"O" document referring to an oral disclosure, use, exhibition or other means</p> <p>"P" document published prior to the international filing date but later than the priority date claimed</p> <p>"T" later document published after the international filing date or priority date and not in conflict with the application but cited to understand the principle or theory underlying the invention</p> <p>"X" document of particular relevance; the claimed invention cannot be considered novel or cannot be considered to involve an inventive step when the document is taken alone</p> <p>"Y" document of particular relevance; the claimed invention cannot be considered to involve an inventive step when the document is combined with one or more other such documents, such combination being obvious to a person skilled in the art</p> <p>"&" document member of the same patent family</p>		
Date of the actual completion of the international search 21 May 1996		Date of mailing of the international search report 18.07.96
Name and mailing address of the ISA European Patent Office, P.B. 5818 Patentlaan 2 NL - 2280 HV Rijswijk Tel. (+ 31-70) 340-2040, Tx. 31 651 epo nl. Fax: (+ 31-70) 340-3016		Authorized officer Ghigliotti, L

INTERNATIONAL SEARCH REPORT

national Application No

PCT/IB 95/00769

C.(Continuation) DOCUMENTS CONSIDERED TO BE RELEVANT

Category *	Citation of document, with indication, where appropriate, of the relevant passages	Relevant to claim No.
A	INTERNATIONAL CONFERENCE ON COMMUNICATIONS, ICC '90. ATLANTA, APR. 15-19, 1990, vol. 4 OF 4, 15 April 1990, INSTITUTE OF ELECTRICAL AND ELECTRONICS ENGINEERS, pages 1742-1746, XP000146075 LIN D. W. ET AL.: "RECEIVER OPTIMIZATION FOR DISPERSIVE CHANNELS EMPLOYING CODED MODULATION, WITH APPLICATION IN HIGH RATE DIGITAL SUBSCRIBER LINE TRANSMISSION" see sections II, III see figure 3 ---	1-24
A	US,A,4 833 693 (EYUBOGLU) 23 May 1989 see column 7, line 67 - column 10, line 8 see figures 1,5 ---	1-24
A	PROCEEDINGS OF THE GLOBAL TELECOMMUNICATIONS CONFERENCE (GLOBECOM), SAN FRANCISCO, NOV. 28 - DEC. 2, 1994, vol. 1 OF 3, 28 November 1994, INSTITUTE OF ELECTRICAL AND ELECTRONICS ENGINEERS, pages 6-10, XP000488508 WANG T. ET AL.: "IMPROVED ADAPTIVE DECISION-FEEDBACK EQUALIZATION WITH INTERLEAVING FOR CODED MODULATION SYSTEMS" see section III see figures 4,5 ---	1-24
A	GB,A,2 286 952 (IBM) 30 August 1995 cited in the application see the whole document -----	1,22

INTERNATIONAL SEARCH REPORT

Information on patent family members

national Application No

PCT/IB 95/00769

Patent document cited in search report	Publication date	Patent family member(s)	Publication date
WO-A-9429989	22-12-94	EP-A- 0704126	03-04-96
US-A-4833693	23-05-89	NONE	
GB-A-2286952	30-08-95	JP-A- 7249998	26-09-95

**This Page is Inserted by IFW Indexing and Scanning
Operations and is not part of the Official Record**

BEST AVAILABLE IMAGES

Defective images within this document are accurate representations of the original documents submitted by the applicant.

Defects in the images include but are not limited to the items checked:

- ☐ **BLACK BORDERS**
- ☐ **IMAGE CUT OFF AT TOP, BOTTOM OR SIDES**
- ☐ **FADED TEXT OR DRAWING**
- ☐ **BLURRED OR ILLEGIBLE TEXT OR DRAWING**
- ☐ **SKEWED/SLANTED IMAGES**
- ☐ **COLOR OR BLACK AND WHITE PHOTOGRAPHS**
- ☐ **GRAY SCALE DOCUMENTS**
- ☐ **LINES OR MARKS ON ORIGINAL DOCUMENT**
- ☐ **REFERENCE(S) OR EXHIBIT(S) SUBMITTED ARE POOR QUALITY**
- ☐ **OTHER:** _____

IMAGES ARE BEST AVAILABLE COPY.

As rescanning these documents will not correct the image problems checked, please do not report these problems to the IFW Image Problem Mailbox.